

## DYNAMIC CRACK PROPAGATION IN ELASTIC- PERFECTLY PLASTIC SOLIDS UNDER PLANE STRESS CONDITIONS

XIAOMIN DENG† and ARES J. ROSAKIS

California Institute of Technology, Pasadena, CA 91125, U.S.A.

(Received 19 April 1990; in revised form 5 July 1990)

### ABSTRACT

THE phenomenon of steady-state dynamic crack propagation in elastic–perfectly plastic solids under mode I plane stress, small-scale yielding conditions is investigated numerically. An Eulerian finite element scheme is employed. The materials are assumed to obey the von Mises yield criterion and the associated flow rule. The ratio of the crack tip plastic zone size to that of the element nearest to the crack tip is of the order of  $1.6 \times 10^4$ . Two subjects of general interest are discussed. These are the asymptotic structure of the crack tip stress and deformation fields, and the appropriateness of a crack growth fracture criterion based on the far-field dynamic stress intensity factor. The crack-line solution by ACHENBACH and LI (Report NU-SML-TR-No. 84-1, Dept. of Civil Engineering, Northwestern University, Evanston, IL 60201, 1984a; in *Fundamentals of Deformation and Fracture* (edited by B. A. BRILBY *et al.*), Cambridge University Press, 1984b) is discussed and compared to the numerical solution. The results of this study strongly indicate that the crack tip strain and velocity fields possess logarithmic singularities, which is consistent with the assumptions in the asymptotic analysis by GAO (*Int. J. Fracture* **34**, 111, 1987). However, it is revealed that the crack tip field variations in Gao's solution present features often contrary to the numerical findings. To this end, a preliminary asymptotic analysis is performed in an effort to resolve certain issues. Finally, the critical plastic strain criterion (McCLINTOCK and IRWIN, in *Fracture Toughness Testing and Its Applications*, ASTM STP 381, p. 84, 1964) is adopted to obtain theoretical relations between the critical dynamic stress intensity factor and the crack propagation speed. These relations are found to agree well with experimental measurements by ROSAKIS *et al.* (*J. Mech. Phys. Solids* **32**, 443, 1984) and by ZEHNDER and ROSAKIS (*Int. J. Fracture*, to appear 1990), performed on thin 4340 steel plates whose material characteristics match those of the calculation. The results seem to support the existence of a one-to-one relationship between the dynamic fracture toughness of the material and the crack propagation speed, for materials which fail in a locally ductile manner.

### 1. INTRODUCTION

THIS finite element study investigates in detail the phenomenon of steady-state dynamic crack propagation in elastic–perfectly plastic solids, under conditions of mode I plane stress and small-scale yielding. Two subjects of general interest are discussed, namely the asymptotic structure of the crack tip fields, and the appropriateness of the dynamic stress intensity factor as a basis for the formulation of a fracture criterion. Results of related numerical studies on crack tip fields in linear

† Present address: Department of Mechanical Engineering, University of South Carolina, Columbia, SC 29208, U.S.A.

hardening and power-law hardening materials, on the effect of non- $K$ -dominance, and on energy dissipation and temperature rise at dynamically propagating crack tips in elastic-plastic solids will be reported separately.

The need to understand the structure of the crack tip field is vital in fracture analyses, and has triggered a large number of analytical and numerical investigations on this subject. For elastic perfectly plastic materials in particular, fairly complete pictures have been achieved for mode III and mode I plane strain crack growth, which were reviewed extensively, for example, by RICE (1982), FREUND (1990) and DENG (1990). For mode I plane stress crack growth, however, this subject still remains elusive.

For quasi-static plane stress crack growth in elastic-perfectly plastic solids, a preliminary analysis was provided by RICE (1982), who demonstrated that only two types of plastic sectors around the crack tip are possible. They are the centered fan sectors and constant stress sectors. Yet no successful attempt in assembling a complete crack tip field has been reported in mode I, even though a solution in mode II was obtained by PONTE CASTAÑEDA (1986). Consequently, the lack of asymptotic solution for mode I plane stress, quasi-static crack growth has forced several investigators to resort to numerical analyses (DEAN, 1983; LUO *et al.*, 1984; NARASIMHAN *et al.*, 1987). These finite element studies conducted under small-scale yielding conditions reveal many interesting features of the crack tip field, but are still not able to completely resolve the detailed structure of the near-tip stress and deformation fields.

A similar situation is encountered for plane stress dynamic crack propagation. To the authors' best knowledge, there is only one asymptotic solution available today (GAO, 1987). Due to mathematical complexities involved in such an asymptotic analysis, it is difficult to judge at the moment as to the appropriateness as well as the correctness of this solution. Moreover, it is our experience from mode III that asymptotic solutions for dynamic crack propagation have a very limited range of dominance at the crack tip, whose size vanishes rapidly as the crack speed goes to zero (FREUND and DOUGLAS, 1982). This fact indicates that a dynamic asymptotic solution cannot capture the full features of the crack tip fields for low and intermediate crack speeds, which seems to diminish its usefulness in the investigation of fracture criteria for crack growth. To this end, full field solutions, such as from a finite element analysis, must be sought. Occasionally, when parameters for fracture criteria are derivable from field variations along the prospective crack line, the so-called crack-line solutions can be used, such as in mode III (FREUND and DOUGLAS, 1982; DUNAYEVSKY and ACHENBACH, 1982). In mode I plane stress, such a solution is offered by ACHENBACH and LI (1984a,b), with the help of an assumption regarding the radial dependence of stresses at the crack front.

The subject of fracture criteria for crack propagation is our next concern. For dynamic crack growth under small-scale yielding conditions the following fracture criterion, based on the far field dynamic stress intensity factor, has been proposed:

$$K_I^d(t) = K_{Ic}^d(v(t)). \quad (1.1)$$

This criterion states that during crack growth, the instantaneous value of the dynamic stress intensity factor  $K_I^d(t)$ , should be, at all times, equal to the quantity  $K_{Ic}^d(v(t))$ ,

called the (plane stress) dynamic fracture toughness. The dynamic fracture toughness is assumed to depend in a one-to-one manner on the crack tip velocity  $v$ . This functional dependence on velocity is expected to be a purely material characteristic.

The appropriateness of the fracture criterion (1.1), or the  $K_{Ic}^d$  vs  $v$  relationship, depends on the assumption that  $K_{Ic}^d$  exhibits a unique, one-to-one dependence on the crack propagation speed. This assumption is a key issue being debated in the dynamic fracture mechanics community today. The debate about the uniqueness of the material dependence of  $K_{Ic}^d(v)$  stems mainly from contradictory experimental observations. For example, while experimental results by KOBAYASHI and DALLY (1977), ROSAKIS *et al.* (1984), and ZEHNDER and ROSAKIS (1990) indicate a unique  $K_{Ic}^d$  vs  $v$  relationship, those by RAVI-CHANDAR (1982), KALTHOFF (1983), and RAVI-CHANDAR and KNAUSS (1987) do not find such a uniqueness.

A closer examination of the experiments reveals that most of the experiments in favor of the uniqueness idea are conducted on metals which fail in a locally ductile manner. Advances in the understanding of crack propagation in such materials have been achieved through some recent studies. In a combined analytical and numerical study of mode III elastic-plastic crack propagation problems, FREUND and DOUGLAS (1982) used a critical plastic strain criterion (MCCLINTOCK and IRWIN, 1964), to obtain theoretical  $K_{Ic}^d$  vs  $v$  curves which resemble those from experiments showing unique  $K_{Ic}^d(v)$  relations. In a separate investigation on the problem of mode I elastic-plastic crack propagation under plane strain, small-scale yielding conditions, LAM and FREUND (1985) employed a different fracture criterion, i.e. the critical crack opening angle criterion (RICE and SORENSEN, 1978; RICE *et al.*, 1980), and again obtained theoretical  $K_{Ic}^d$  vs  $v$  curves with the same qualitative tendencies. It should be noted here that these criteria are mostly suited for metals that fail in a locally ductile manner.

Although the above comparisons are made between theoretically generated  $K_{Ic}^d$  vs  $v$  curves for mode III and mode I plane strain, and experimental results which are more closely related to mode I plane stress, such comparisons do strongly indicate that it is indeed possible to explain experimental observations in terms of local material behavior at the crack tip. Since many engineering structures are made of thin sheets, a plane stress elastic-plastic analysis, such as the present study, is also necessary. Furthermore, due to the complicated three-dimensional character of the stress and deformation fields near the crack edge, detailed two-dimensional analyses, whether in plane stress or plane strain, or in anti-plane shear, are the first step towards the full understanding of the three-dimensional fracture behavior. However, also due to the three-dimensional character of the near-tip fields, all such two-dimensional analyses are bound to be qualitative in nature, and findings of such analyses must be interpreted cautiously.

The finite element formulation employed in this study is of the Eulerian type, which was first used in fracture mechanics by DEAN and HUTCHINSON (1980). Stresses are obtained by numerically integrating the incremental elastic-plastic constitutive law over strain increments, with the Modified Tangent Predictor-Radial Return algorithm (DENG, 1990). This stress integration algorithm combines the fine points of both the original Tangent Predictor-Radial Return algorithm (SCHREYER *et al.*, 1979), and the Secant Stiffness algorithm (RICE and TRACEY, 1973; TRACEY, 1976), in that it is easy to implement in plane stress, and that it gives a stress state automatically satisfying

the yield condition at the end of a strain increment for elastic–perfectly plastic and linear hardening materials.

In implementing the stress integration algorithm, a solution procedure proposed by DENG and ROSAKIS (1990) is adopted. With this technique, existing solution procedures in wide use today can be modified to eliminate the occurrence of negative plastic flow, and to avoid treating elastic unloading as plastic flow. This modification is shown to improve the accuracy and convergence of the numerical solution.

## 2. FINITE ELEMENT FORMULATION

In this section, the finite element formulation and the design of the finite element mesh are discussed briefly. Details can be found in other publications (DENG, 1990; DENG and ROSAKIS, 1990).

The elastic–perfectly plastic material under consideration is assumed to be homogeneous, isotropic and obey the von Mises yield condition and the associated flow rule. Suppose a crack is propagating steadily in a plate made of such a material (refer to Fig. 1), such that an observer moving with the crack tip will not see any changes of the crack tip fields as the crack extends. Mathematically, this requires that the crack speed  $v$  be a constant, and that for any field quantity, say,  $q$ , its material time derivative be computed from

$$\frac{\partial q}{\partial t} = -v \frac{\partial q}{\partial x_1}. \quad (2.1)$$

Equation (2.1) implies that the time rate or the time history of any field quantity for steady-state crack growth is stored spatially along horizontal lines parallel to the direction of crack propagation.

Making use of the property specified by (2.1) for steady-state crack growth, an iterative finite element solution procedure proposed by DEAN and HUTCHINSON (1980) is adopted in this study. At each solution step, convergence is said to have been

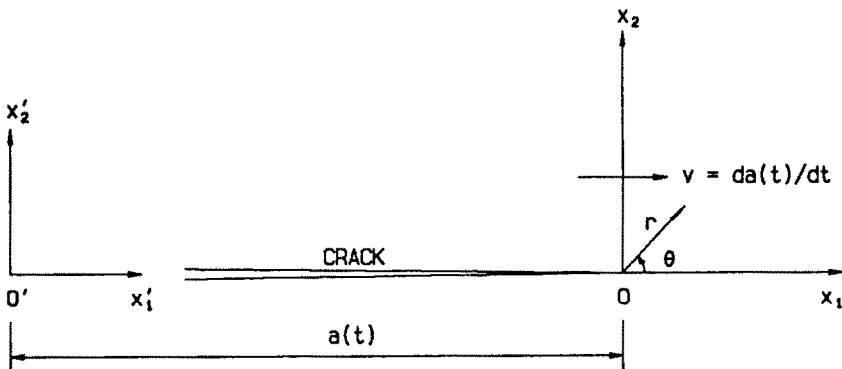


FIG. 1. A diagram of crack propagation, where  $(x'_1, x'_2)$  is a fixed reference coordinate system,  $(x_1, x_2)$  is a moving system with origin at the crack tip, and  $(r, \theta)$  is the associated polar coordinate system.

reached at the  $(k+1)$ th iteration, if the following criterion is met simultaneously for every choice of  $i, j$  and  $\alpha$ :

$$\frac{\|\sigma_{ij}^{k+1} - \sigma_{ij}^k\|_2}{\|\sigma_{ij}^{k+1}\|_2} \leq \epsilon, \quad (2.2a)$$

$$\frac{\|\epsilon_{ij}^{k+1} - \epsilon_{ij}^k\|_2}{\|\epsilon_{ij}^{k+1}\|_2} \leq \epsilon, \quad (2.2b)$$

$$\frac{\|u_\alpha^{k+1} - u_\alpha^k\|_2}{\|u_\alpha^{k+1}\|_2} \leq \epsilon, \quad (2.2c)$$

where  $\sigma_{ij}$ ,  $\epsilon_{ij}$  and  $u_\alpha$  represent respectively the stress, strain and displacement components,  $i, j$  have the values of 1, 2 and 3,  $\alpha$  has the values of 1 and 2,  $\|\bullet\|_2$  is the standard 2-norm, and  $\epsilon$  is the error tolerance which is a small positive number. The stress and strain norms are summed over all Gauss integration points, and the displacement norm is summed over all nodal points. The value of  $\epsilon$  is taken to be around  $1.0 \times 10^{-4}$  in the current computation.

In this investigation, the small-scale yielding condition (RICE, 1967, 1968) is assumed. A rectangular domain of finite size (see Fig. 2) is used to model the mathematical problem of a semi-infinite crack advancing in an otherwise infinite plate.

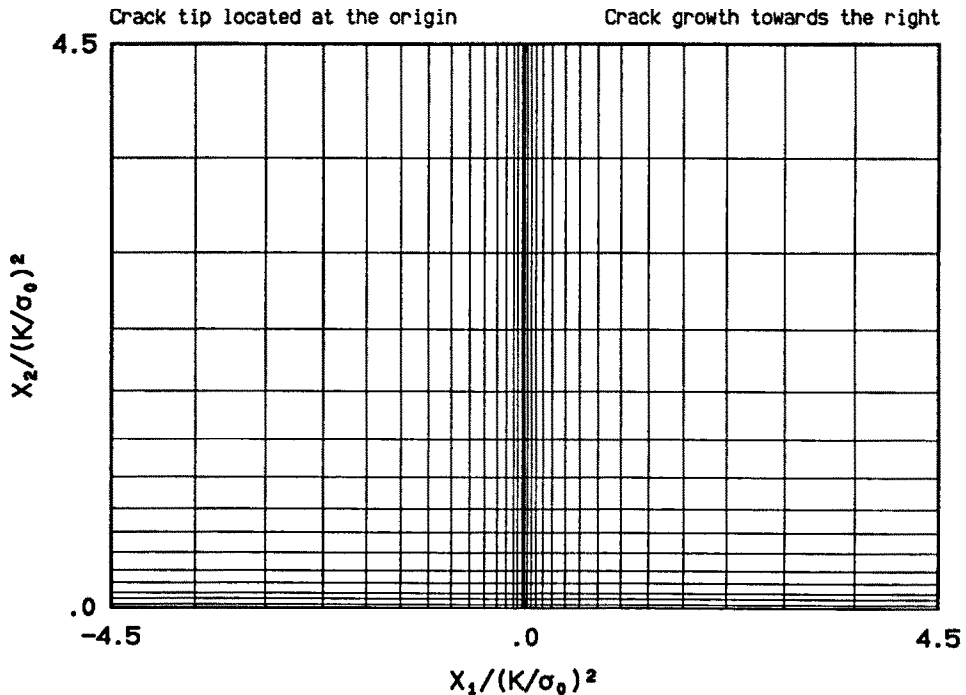


FIG. 2. A coarse representation of the finite element mesh used in the present computation.

According to the boundary layer concept introduced by RICE (1967, 1968), the solution for this mathematical problem is equivalent to the crack tip solution for the original mechanics problem under small-scale yielding conditions. As pointed out by DEAN (1983), a domain with a size larger than 10 times that of the crack tip active plastic zone will suffice to produce reasonable results. The size employed in this investigation is about 15 times larger than that of the plastic zone.

The middle point of the rectangle's bottom boundary is made to coincide with the current crack tip position. The traction-free crack surface lies along the bottom from the lower left corner to the crack tip; accordingly, the line from the crack tip to the lower right corner represents the symmetry plane. Also from the schematic of the mesh shown in Fig. 2, it is seen that the rectangle is discretized by a network of horizontal and vertical lines, whose intervals decrease rapidly towards the bottom line and the center vertical line, resulting in increasingly small elements near the crack tip. The divided areas are simply represented by four-noded isoparametric rectangular elements, with  $2 \times 2$  Gauss integration points. This type of element arrangement is designed to fit the need of the Eulerian finite element formulation, such that stresses can be integrated along horizontal lines composed of Gauss points, from the right boundary to the left (for details, see DENG, 1990).

Two meshes of high resolution are used in our computation. They are different in that the numbers of the horizontal and vertical lines of the mesh networks and the variations of the intervals between those lines are different. In the finer mesh, the network of lines results in 4050 elements with 4186 nodes, and the ratio of the plastic zone size to that of the smallest near-tip element is of the order of  $1.6 \times 10^4$ . In the slightly coarser mesh, there are 1800 elements, and the plastic zone size is about  $0.8 \times 10^4$  times the size of the smallest near-tip element. Comparisons between numerical results obtained from those two meshes demonstrate very good agreement, which will be discussed in the next section.

The boundary condition is specified as follows. In accordance with the small-scale yielding assumption, surface tractions and displacements corresponding to the crack tip elastic singular field, which is characterized uniquely by the dynamic stress intensity factor  $K_I^d$ , are prescribed on the domain boundary, with necessary updating on the portion of the boundary near the crack flank, where boundary conditions incompatible with the  $K$ -field arise due to the presence of the residual plasticity in the plastic wake. The Poisson ratio  $\nu$  is taken to be 0.3. All logarithmic values used in figures are based on the natural number  $e$ .

### 3. CRACK TIP FIELDS

Crack tip asymptotic fields for quasi-static crack growth under conditions of mode I plane stress and small-scale yielding is first explored. This subject was previously investigated, using the finite element method, by DEAN (1983), LUO *et al.* (1984), and NARASIMHAN *et al.* (1987), which revealed many features of the crack tip fields. Since a much finer mesh is employed in the present study, and from detailed comparisons performed in DENG (1990), we believe that the results of the current study represent a better approximation for steady-state quasi-static crack tip fields.

However, most of the results regarding quasi-static crack growth obtained in this study will not be cited here, but can be found in DENG (1990), which documents numerical field variations and analytic asymptotic analyses not yet published in the literature.

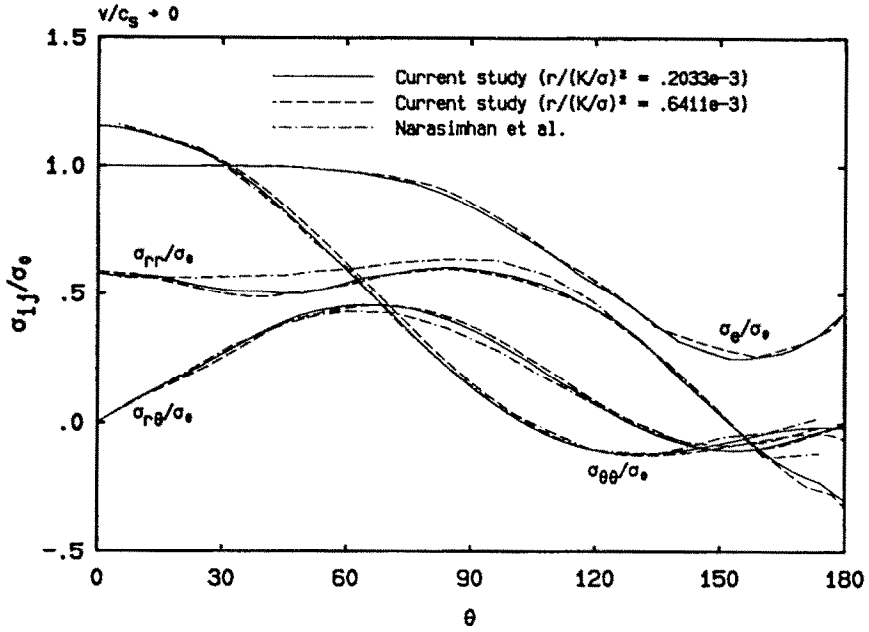
Nonetheless, to indicate the accuracy and reliability of this study, a brief comparison of results is made below, with those by NARASIMHAN *et al.* (1987), who adopted a totally different finite element formulation, namely the nodal release procedure first used by SORENSEN (1978). The comparisons are shown in Fig. 3, with  $\sigma_0$  and  $\tau_0$  denoting respectively the initial yield stress in tension and shear, which indeed demonstrate very good overall agreement. Note that in the angular variations, numerical data are taken along a rectangular path about  $1.0 \times 10^{-2}(K/\sigma_0)^2$  away from the crack tip in the results of Narasimhan *et al.*, and along circular paths in the current study, where the path with radius  $r/(K/\sigma_0)^2 = 0.6411 \times 10^{-3}$  is for the coarser finite element mesh, and the path with radius  $r/(K/\sigma_0)^2 = 0.2033 \times 10^{-3}$  is for the finer mesh. Further confidence in the results of the present study can be gained through detailed comparisons, between available asymptotic analyses and parallel finite element studies by the current authors, of asymptotic crack tip stress and velocity field variations for quasi-static and dynamic crack growth in linear hardening solids under plane stress conditions. These comparisons, which will be reported separately and can be found in DENG (1990), demonstrate very good agreement.

Published studies on the stress and deformation fields around a rapidly propagating crack tip in an elastic-perfectly plastic solid under plane stress or generalized plane stress conditions are rare.

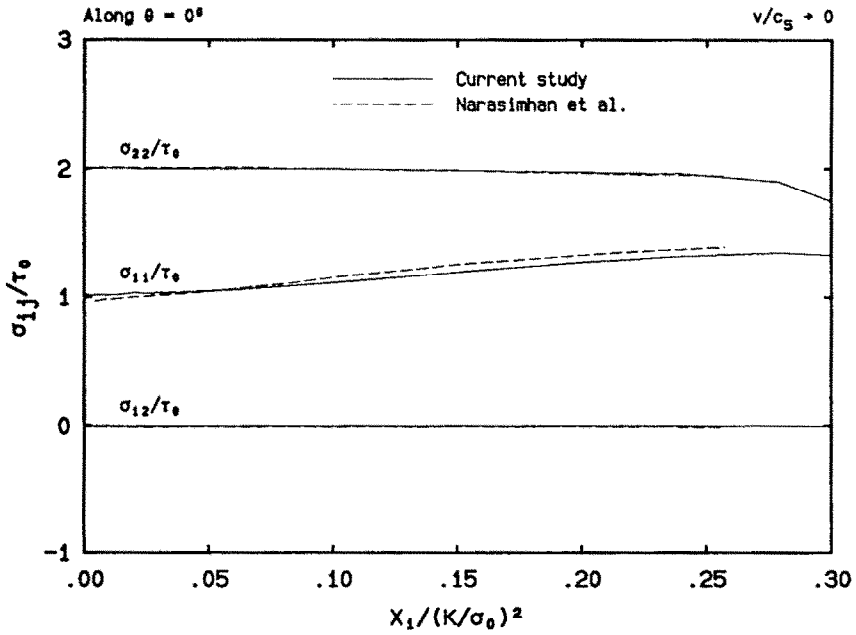
ACHENBACH and LI (1984a,b) proposed a crack-line solution for mode I steady-state which assumes that  $\sigma_{22}$  and hence  $\sigma_{11}$  are constant along  $\theta = 0^\circ$  from the crack tip up to the elastic-plastic boundary, which is then used to extract a theoretical  $K_{Ic}^d$  vs  $v$  curve, where  $K_{Ic}^d$  is the plane stress fracture toughness, and  $v$  the crack tip speed. However, to interpret their findings correctly, it is necessary to verify the assumptions which form the very basis of their analysis. There are no such verifications available as of today.

GAO (1987), on the other hand, obtained an analytic mode I solution valid asymptotically in the crack tip area. Due to the mathematical complexities involved in the analysis and due to the limited data presented in his paper, it is difficult to judge with confidence whether this solution is unique or appropriate. Besides, from the experience for mode III fracture, it is expected that any first-order asymptotic dynamic solution would only have a restricted near-tip domain of validity which vanishes as the crack tip velocity goes to zero. This poses a problem when one is interested in getting a crack-velocity dependence for a certain physical quantity, say, for the dynamic fracture toughness.

It is apparent then that detailed full field numerical studies will greatly help to resolve the issues mentioned above. To our best knowledge, the results presented in the following document are the first published effort to investigate numerically the crack tip stress and deformation fields for dynamic elastic-plastic crack growth under plane stress conditions. The two meshes, both of high spatial resolution, are used as follows. The finer mesh is employed to study a typical dynamic case, namely the case for  $m = 0.3$ , where  $m$  is the ratio of the crack tip speed  $v$  to the material elastic shear



(a)



(b)

FIG. 3. (a) Angular variations of the effective stress and the polar stress components, compared with the results by NARASIMHAN *et al.* (1987). (b) Detailed view of the radial dependence of the stress components at crack front, compared with the results by NARASIMHAN *et al.* (1987).

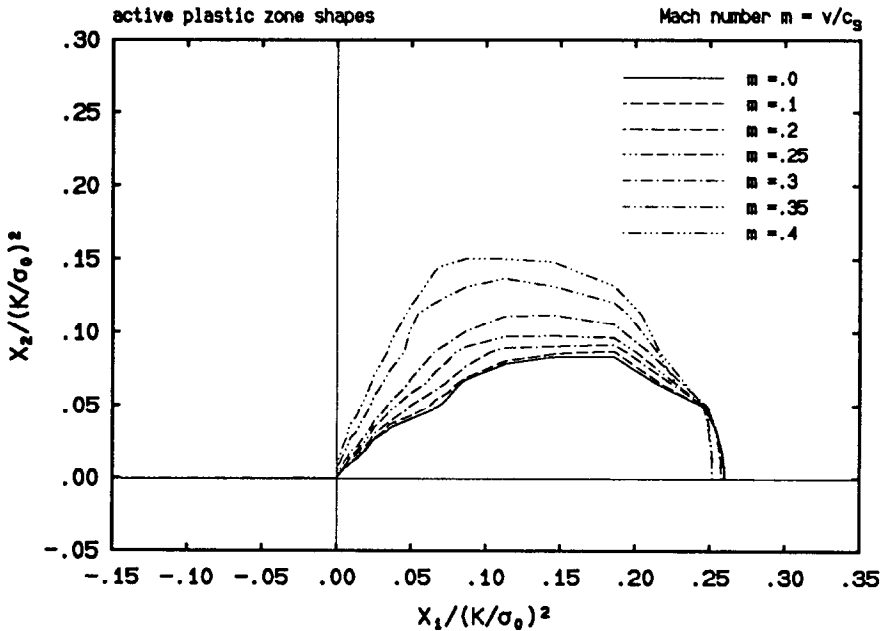
wave speed  $c_s$ . The slightly coarser mesh is used, for cost considerations, to carry out computations for the whole range of  $m$  values from 0.0 to 0.4, where quasi-static crack growth is meant by  $m = 0$ . The evolutionary variations of field quantities with respect to  $m$  are thus obtained.

*The active plastic zones*

The variation of the active plastic-zone shapes with respect to the Mach number  $m$  is shown in Fig. 4(a), where the coordinates are nondimensionalized through the usual normalization  $(K/\sigma_0)^2$ , with  $K$  being the generic dynamic stress intensity factor, and  $\sigma_0$  the initial yield stress in tension.

It is observed that as  $m$  or the normalized crack speed increases, the active plastic zone shrinks along the crack line from size  $0.265(K/\sigma_0)^2$  at  $m = 0.0$  to  $0.255(K/\sigma_0)^2$  at  $m = 0.4$ , and it spreads out in its height direction from size  $0.084(K/\sigma_0)^2$  to about  $0.15(K/\sigma_0)^2$ , which almost doubles the quasi-static value.

Moreover, the near-tip angular extent of the active plastic zone grows as  $m$  becomes larger, actually from  $45^\circ$  at  $m = 0.0$  to about  $90^\circ$  at  $m = 0.4$ , as shown by an expanded view of the crack tip zone in Fig. 4(b). From this figure, a secondary active plastic



(a)

FIG. 4. (a) Active plastic zone shapes for various normalized crack propagation velocities, with the origin located at the crack tip. (b) Detailed view of the active plastic zone shapes at the crack tip for various normalized crack propagation velocities, with the origin located at the crack tip. (c) The variations of the angular extent of the near-tip active plastic zones with respect to the normalized crack speed.

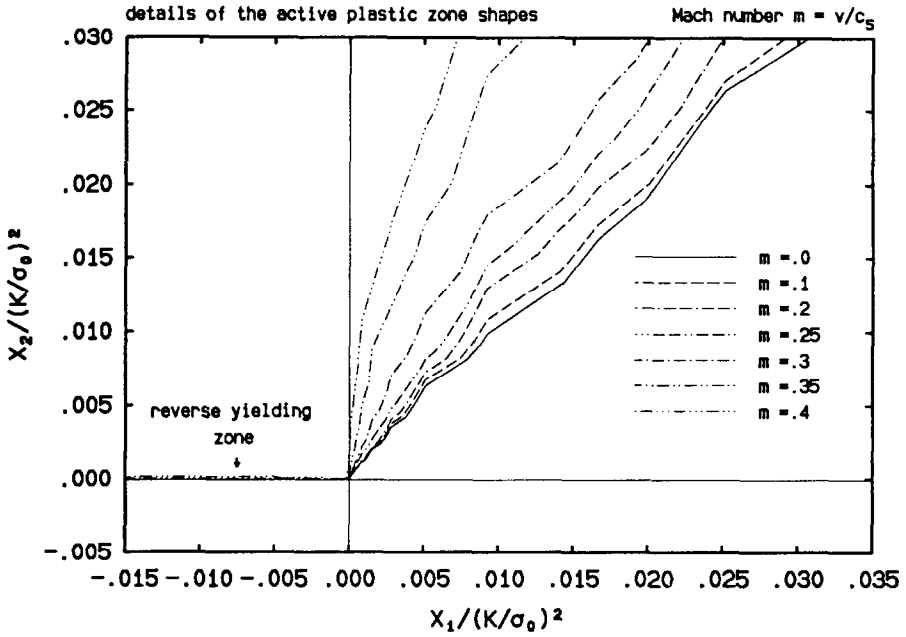


FIG. 4(b).

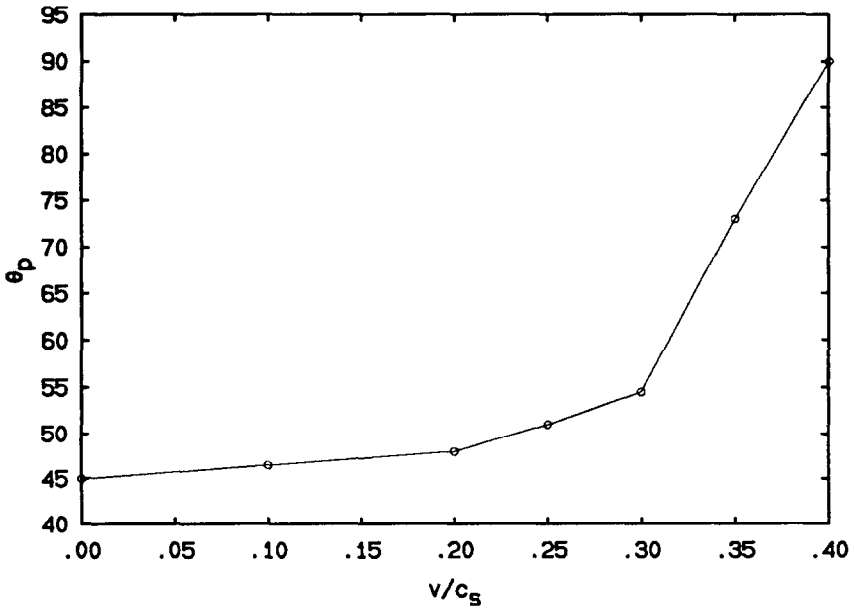


FIG. 4(c).

zone, or a reversed yielding zone, is clearly revealed for  $m = 0.35$  and  $0.4$  near the crack flank. The variations of the angular extent of the primary near-tip active plastic zones with respect to  $m$  is shown in Fig. 4(c).

This type of plastic zone arrangement is very similar to the findings of DOUGLAS (1981) for mode III dynamic crack propagation, utilizing the same finite element technique as used in this study. While the asymptotic solution by SLEPYAN (1976) for mode III predicts an all-round plastic zone, which is not confirmed by Douglas' investigation, Gao's mode I plane stress asymptotic solution anticipates an elastic unloading sector behind the primary active plastic zone, which is consistent with our results.

*Angular field variations*

As in the quasi-static case, our angular field variations are obtained from finite element data extracted from locations about five elements away from the crack tip along a circular path with a distance to the tip of  $0.2033 \times 10^{-3} (K/\sigma_0)^2$  for the finer mesh, which is about one thirteen-hundredth of the active plastic zone size  $R_p$ , and of  $0.6411 \times 10^{-3} (K/\sigma_0)^2$  for the coarser mesh, which is about one four-hundredth of  $R_p$ .

In conjunction with the above-observed reverse yielding phenomenon, the angular effective stress distribution presented in Fig. 5(a) gives details regarding the evol-

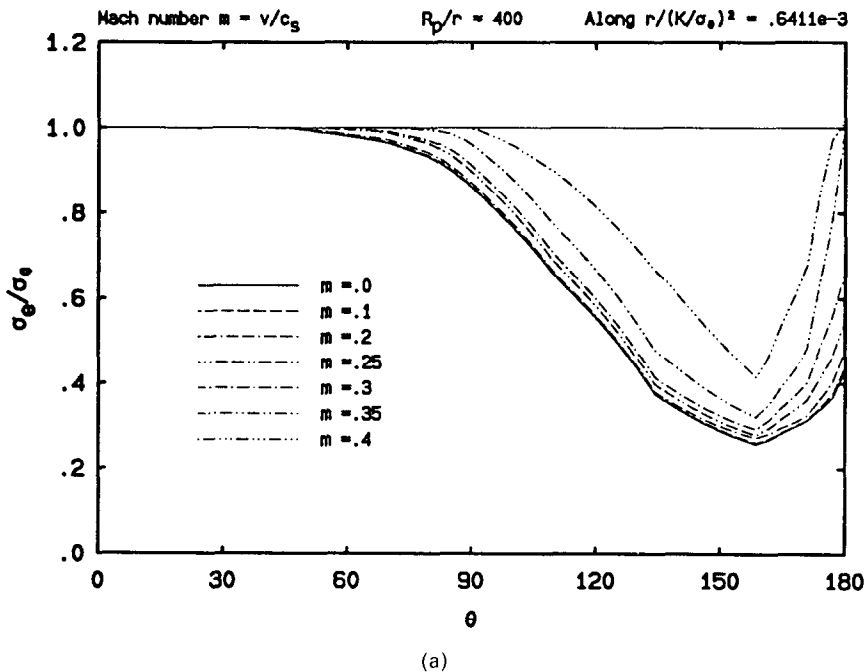


FIG. 5. (a) The angular dependence of the effective stress for various normalized crack speeds. (b) The angular dependence of the polar stress components for various normalized crack speeds. (c) The angular dependence of the Cartesian rectangular stress components for  $v/c_s = 0.3$ .

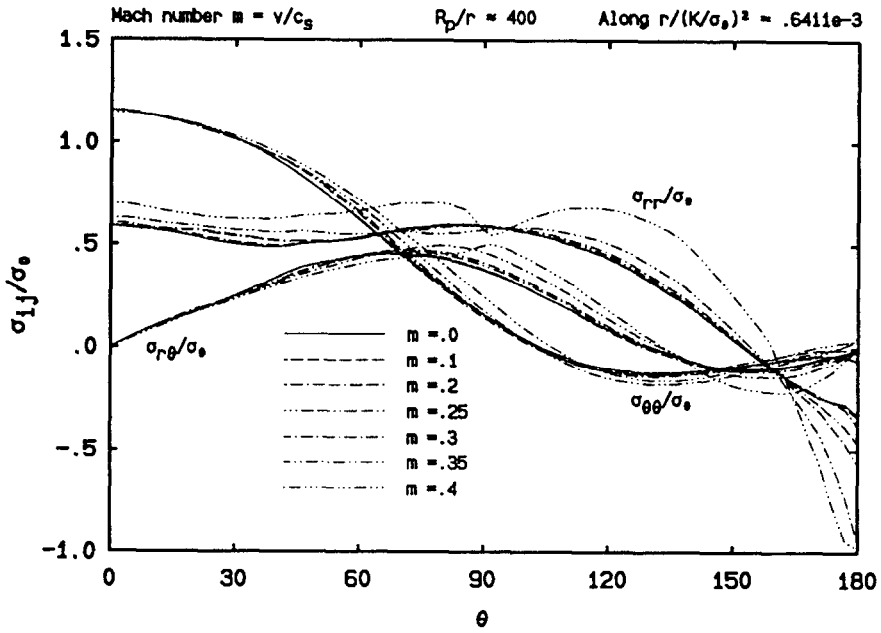


FIG. 5(b).

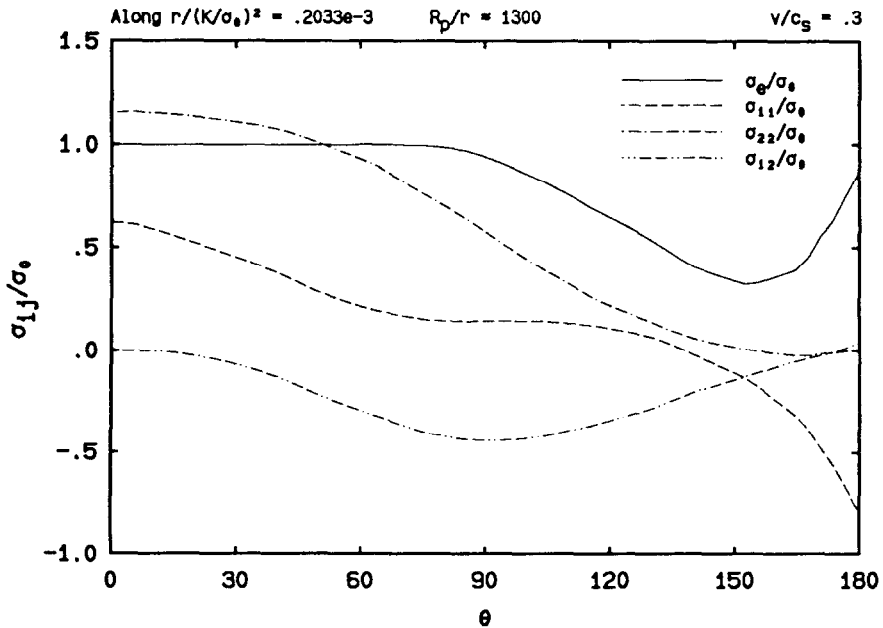


FIG. 5(c).

utionary tendency of the existence of a secondary active plastic zone behind the crack tip, where  $\sigma_e$ , the effective stress, regains its yielding value  $\sigma_0$  for  $m = 0.35$  and  $0.40$ . The asymptotic solution by GAO (1987) shows however that the secondary active plastic zone exists for all values of  $m$  from  $0.0$  to  $0.3$ . In particular, he found that the angular extent of this reverse yielding zone increases as  $m$  decreases, which is strongly contrary to our findings.

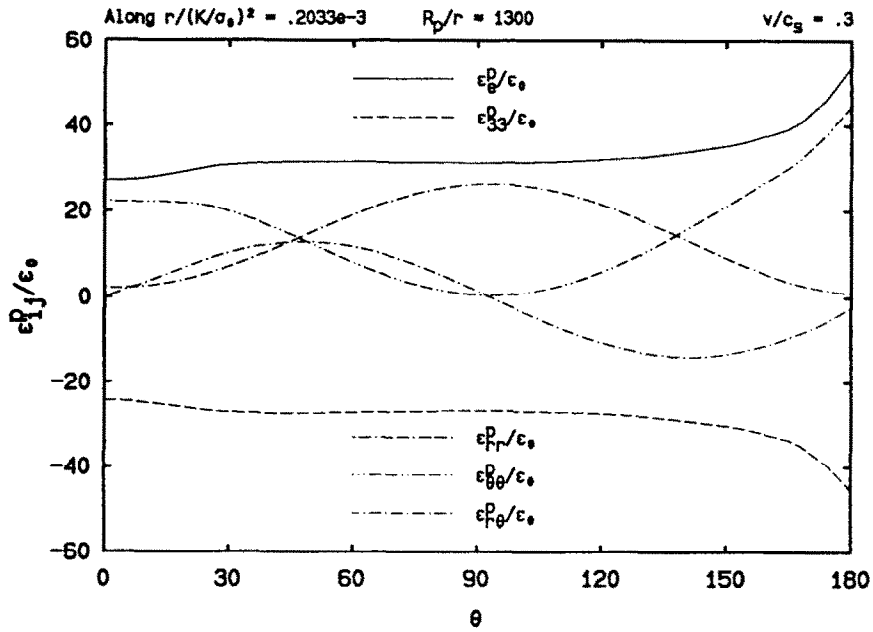
Figure 5(a) also reveals that the effective stress deviates from  $\sigma_0$  at about  $\theta = 45^\circ$  for  $m = 0.0$ , and  $90^\circ$  for  $m = 0.4$ , which are consistent with our earlier discoveries pertaining to the angular extent of the primary active plastic zones at the crack front. Again Gao's results predict different active plastic zone angles, which, in his calculation, are always larger than  $90^\circ$ .

Next we discuss, as shown in Fig. 5(b), the  $\theta$ -dependence of other stress components. First we want to point out that the symmetry condition at the crack front and the traction-free condition at the crack faces are well satisfied. We emphasize this because with the Eulerian-type finite formulation we employed, stresses are obtained through integration of the incremental constitutive law, along lines parallel to the crack line, from crack front downstream to the area behind the crack tip. When the integration sweeps the crack tip, the inevitable large discretization errors at the crack tip are carried over to regions behind. It is then expected that such numerical errors are accumulated along the crack flank and the momentum-balance iterations are mostly carried out to minimize the errors there. Hence the satisfaction of the boundary conditions at the crack surface is a major indication of a converged numerical solution.

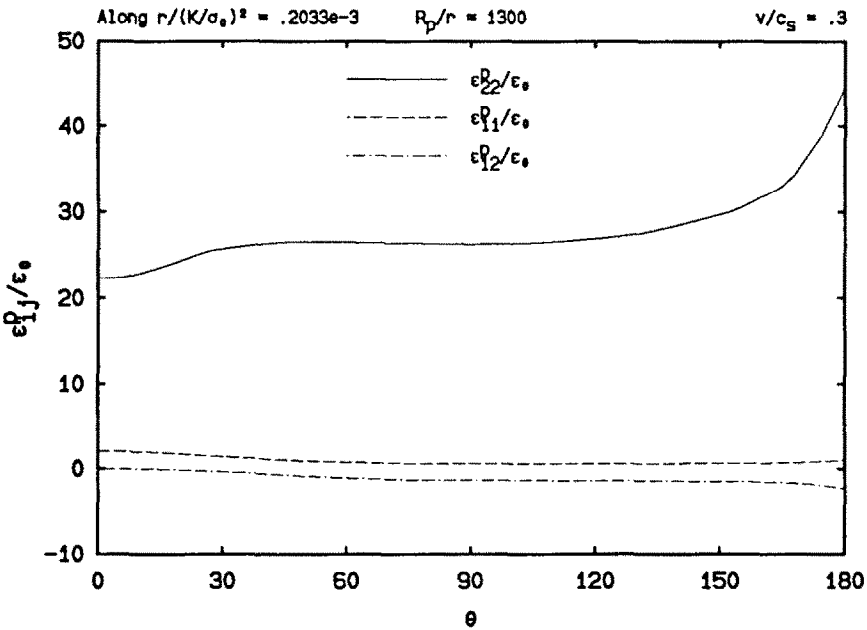
It is then seen from Fig. 5(b) that the changes of  $\sigma_{\theta\theta}$  with respect to  $\theta$  are smooth for all values of  $m$ , and that while the changes of  $\sigma_{rr}$  and  $\sigma_{r\theta}$  are smooth for lower  $m$  values, a kink develops for higher  $m$  values, notably for the case of  $m = 0.4$  at  $\theta \doteq 90^\circ$ , where approximately the boundary between the active plastic zone and the elastic unloading zone is located. This seems to agree qualitatively with the analytic predictions by GAO (1987) although quantitatively large differences exist.

The angular variations of the Cartesian rectangular stress components are shown in Fig. 5(c), for the typical case of  $m = 0.3$ . It is found that  $\sigma_{22}$  and  $\sigma_{12}$  are respectively always positive and negative except near the crack surface, whereas  $\sigma_{11}$  changes sign when  $\theta$  reaches approximately  $135^\circ$ .

Next the plastic strain variations are illustrated, with strains normalized by  $\varepsilon_0$ , the initial yield strain in tension. It is noted that the plastic strains outside the active plastic zones are the residual plastic strains. Figure 6(a) shows the  $\theta$ -dependence of the polar components of the plastic strain, the effective plastic strain and the out-of-plane plastic strain for  $m = 0.3$ . It is seen that the polar components exhibit, just as in the quasi-static case, sinusoidal-like behaviors while  $\varepsilon_\theta^\theta$  and  $\varepsilon_{33}^3$  remain fairly flat for most of the  $\theta$  ranges and rise up near the crack flank, which are apparently due to the residual plastic strains accumulated at the crack tip (theoretically they should tend to infinity if the plastic strains in the active plastic zone are singular). The sinusoidal-like behaviors are in fact present in all our calculated cases, whose progressive changes with respect to  $m$  are shown in DENG (1990). This phenomenon is easily explained if the angular variations of the Cartesian rectangular plastic strain components are examined. It is discovered from Fig. 6(b), for the case of  $m = 0.3$ , that throughout the angular range, the 2-2 component is dominantly larger than the



(a)



(b)

FIG. 6. (a) The angular dependence of the effective plastic strain, the out-of-plane plastic strain and the polar plastic strain components for  $v/c_s = 0.3$ . (b) The angular dependence of the Cartesian rectangular plastic strain components for  $v/c_s = 0.3$ .

1-1 and 1-2 components, which means that the effective plastic strain, through its definition, and the out-of-plane plastic strain, through the plastic incompressibility, are dominated by  $\epsilon_{22}^p$ . Hence, they behave like  $\epsilon_{22}^p$  as seen from the figures. The predominance of the 2-2 Cartesian component certainly also accounts for the sinusoidal behaviors of the polar components, which becomes clear if a tensorial transformation is performed. It is also worth mentioning that as the crack speed goes up, the magnitude of  $\epsilon_{22}^p$  decreases and that of  $\epsilon_{11}^p$  increases.

The angular variations of the velocity field around the crack tip are shown in Fig. 7(a) for the polar components and in Fig. 7(b) for the Cartesian components. It is observed that  $v_r$  starts negatively at  $\theta = 0^\circ$  and ends at values close to zero, whereas  $v_\theta$  starts at zero, as it should due to symmetry conditions, and ends at negative values. For all  $m$  values we considered, both  $v_r$  and  $v_\theta$  curves go up steadily (i.e. with positive slopes) initially and then fall down consistently all the way to the crack surface. The Cartesian components also share the initial positive-slope characteristic and remain that way approximately up to the elastic-plastic boundary where they level off until they meet the crack surface.

We would like to emphasize the observation that at  $\theta = 180^\circ$   $v_1$  is very close to zero for  $m < 0.3$ , and it apparently becomes nonzero as  $m$  becomes larger, especially for  $m = 0.4$ , which, in our opinion, has to do with the fact that as  $m$  becomes larger, a secondary active plastic zone develops along the crack flank.

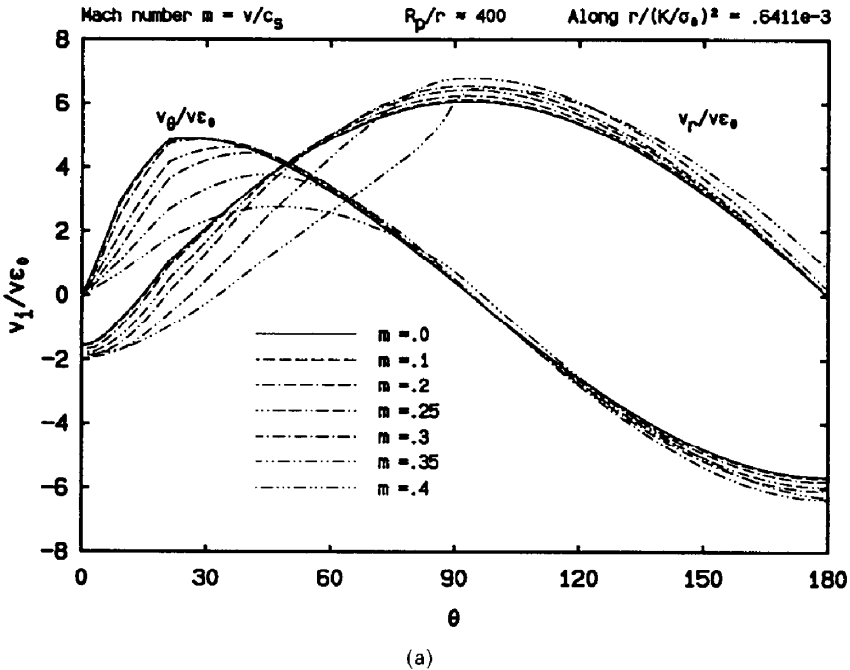


FIG. 7. (a) The angular dependence of the polar velocity components for various normalized crack speeds. (b) The angular dependence of the Cartesian velocity components for various normalized crack speeds.

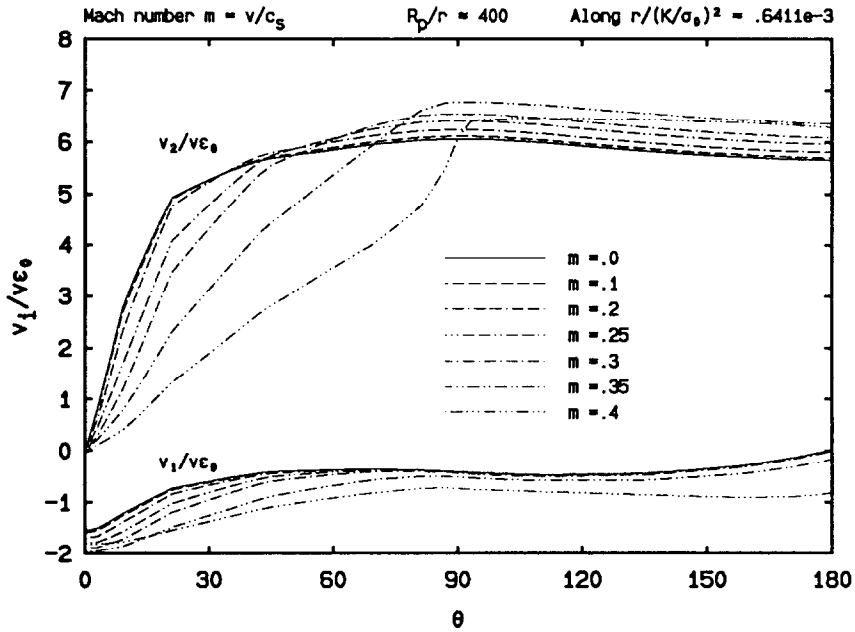


FIG. 7(b).

We will show in the subsection of asymptotic analysis that if there is no plastic reloading at the back of the crack tip, then inside the elastic unloading zone behind the crack tip,  $v_1$  is less singular than  $\ln r$  whereas  $v_2$  is as singular as  $\ln r$ , which means that the magnitude of  $v_1$  there is vanishingly small when compared with that of  $v_2$ . However, if there is a plastic reloading zone at the back of the crack tip, then both  $v_1$  and  $v_2$  should possess the same  $\ln r$  singularity as  $r$  approaches zero, but the coefficient for the  $v_1$  singularity is not necessarily zero.

### Radial field variations

Many interesting characteristics can be observed from the radial distributions of stress and deformation fields, which are also very important for the studies of fracture criteria and for the search of appropriate asymptotic solutions.

Figure 8(a) describes for  $m = 0.3$  the crack-front stress variations with respect to the normalized radial distance and covering regions both inside and outside the plastic zone. It is obvious from the figure that outside the plastic zone (note that the plastic zone size is about  $0.26(K/\sigma_0)^2$ ) both  $\sigma_{11}$  and  $\sigma_{22}$  become smaller as the distance from the crack tip becomes larger, and eventually they intersect each other and then change their relative magnitudes as required by the dynamic asymptotic  $K$ -field specified on the crack-front boundary. While inside the plastic zone, it is seen that as the distance increases,  $\sigma_{11}$  increases sharply whereas  $\sigma_{22}$  only decreases slightly, and that  $\sigma_{11}$  has a crack tip asymptotic value clearly greater than  $\tau_0$ , i.e. greater than its quasi-static

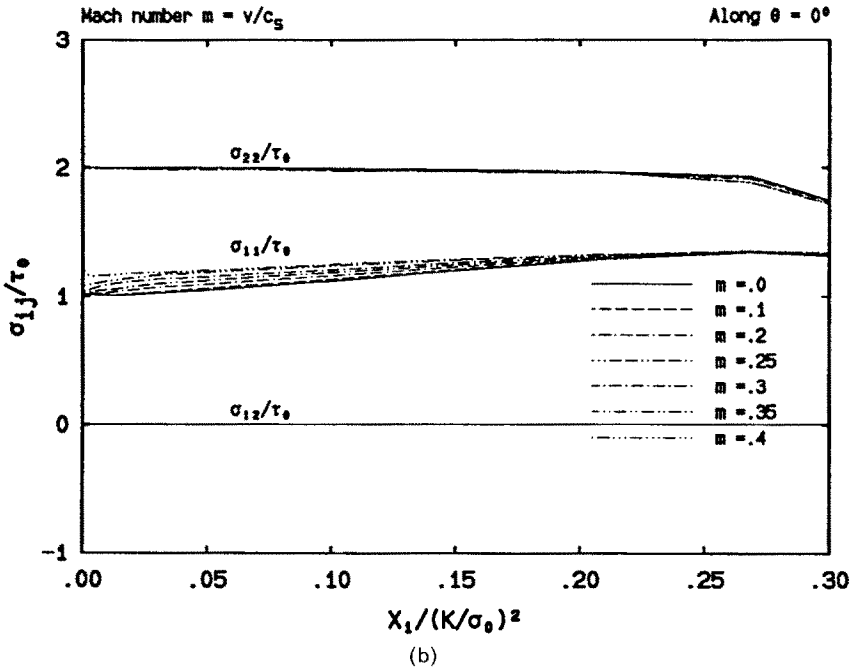
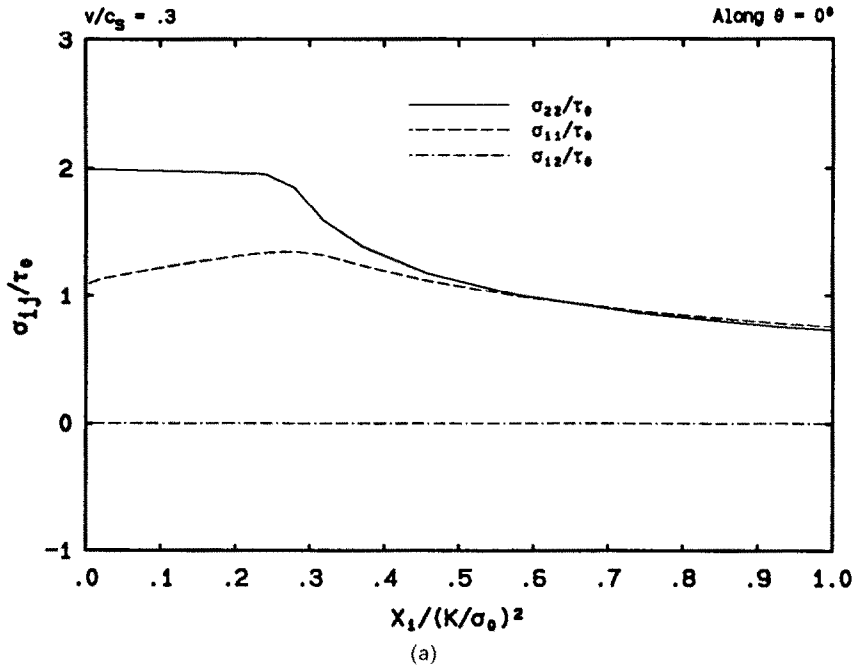


FIG. 8. (a) The radial dependence of the stress components at the crack front along the prospective crack line for  $v/c_s = 0.3$ . (b) The radial dependence of the stress components at the crack front for various normalized crack speeds. (c) The radial dependence of the 2-2 stress component at the crack front for various normalized crack speeds.

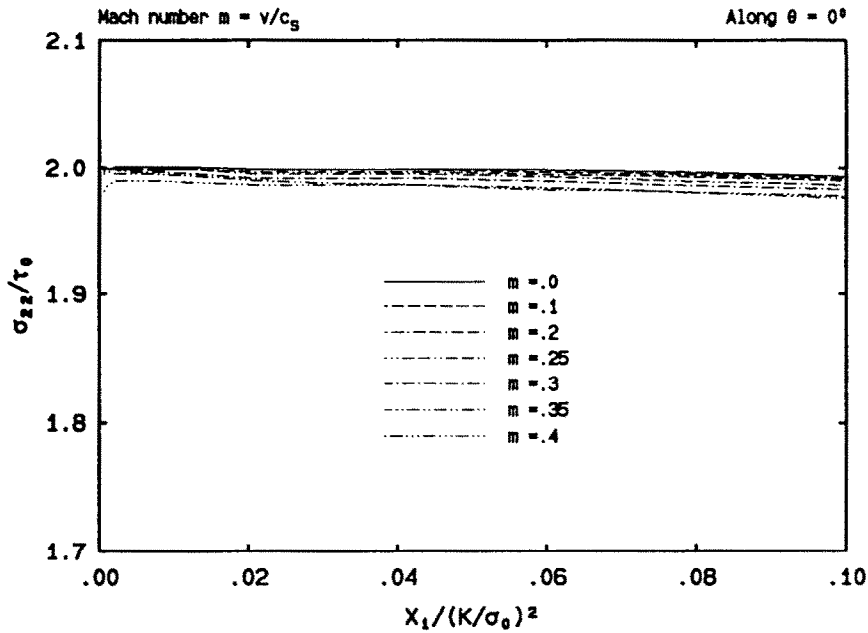


FIG. 8(c).

counterpart, whereas  $\sigma_{22}$  has an asymptotic value about  $2\tau_0$  which is almost the same as the quasi-static value.

A more detailed asymptotic view of the radial stress distributions along the crack line is presented in Fig. 8(b,c) for all cases of crack propagation speeds considered. It is discovered that while  $\sigma_{11}$  increases as  $m$  goes up (see Fig. 8b),  $\sigma_{22}$  actually decreases, although slightly, as  $m$  increases.

At this point we would like to point out a strong inconsistency of the solution by GAO (1987) with our numerical findings. It can be seen from Figs 3 and 4 of Gao's paper that the value of  $\sigma_{11}$  at  $\theta = 0^\circ$  for  $m = 0.3$  is smaller than  $\tau_0$ , or smaller than that for  $m = 0$  (also refer to Fig. 5 of his paper).

Our numerical solutions also showed approximate linear radial variations of both  $\sigma_{11}$  and  $\sigma_{22}$ . Note also that the 1-2 component of the stress field is always zero, satisfying the symmetry condition at  $\theta = 0^\circ$ .

The strong  $r$ -dependence of the 1-1 stress component noted in Fig. 8(a,b) is apparently in disagreement with the assumption made in the crack-line solutions by ACHENBACH and LI (1984a,b), namely the assumption that  $\sigma_{22}(r)$  and hence  $\sigma_{11}(r)$  are constants along  $\theta = 0$  up to the elastic-plastic boundary.

The radial dependence of crack tip plastic strains is shown in Figs 9-12. First of all, typical variations are illustrated along the radial line  $45^\circ$  which are depicted in Fig. 9, where we see that very near the crack tip, the 2-2 plastic strain component,

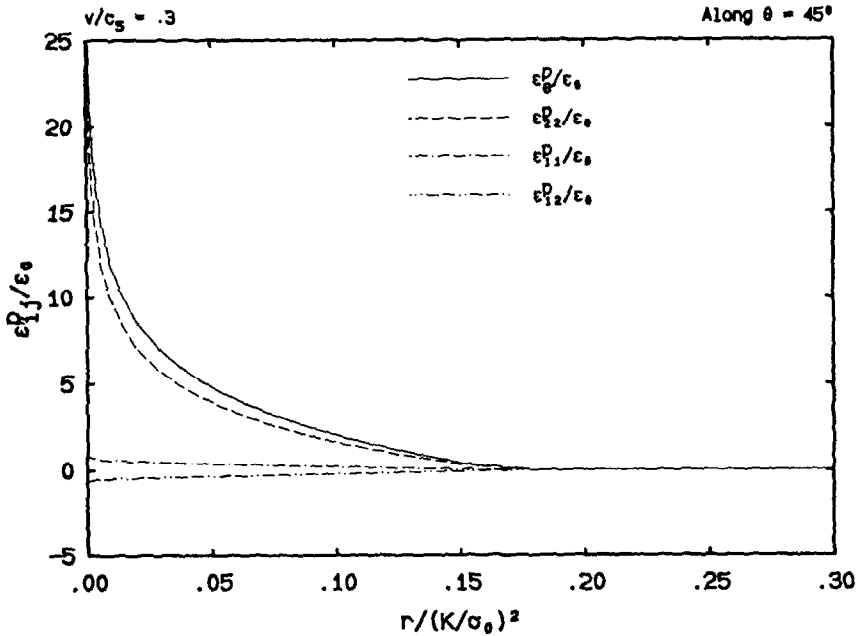


FIG. 9. The radial dependence of the Cartesian rectangular plastic strain components along the radial line  $\theta = 45^\circ$  for  $v/c_s = 0.3$ .

and hence the effective plastic strain, demonstrate much stronger radial dependence than the 1-1 and 1-2 components, which confirms our earlier observations from their angular variations (see Fig. 6). However we cannot rule out the possibility that  $\epsilon_{11}^p$  and  $\epsilon_{12}^p$  are singular as  $r \rightarrow 0$ , although their magnitudes will be very small compared to the magnitude of  $\epsilon_{22}^p$ .

The 1-1 plastic strain component variations for various  $m$  values are illustrated in Fig. 10. It is clear from the figure that  $\epsilon_{11}^p$  does show large slopes near the crack tip, especially for larger  $m$  values, which indicates a singular behavior. In fact, if the data in Fig. 10 are plotted in log-coordinates, approximate linear relations can be observed, which strongly suggests a logarithmic singularity. Another characteristic of the 1-1 component variation is that its magnitude tends to flip over to lower values as the normalized distance increases, which can be seen from Fig. 10.

The evolutionary variations of  $\epsilon_{22}^p$  along the crack line is shown in Fig. 11(a). One of the characteristics of these variations is that as  $m$  increases, the magnitude of this dominant plastic strain component decreases. It is observed that a clear singularity exists at the crack tip. Actually it is strongly indicated in Fig. 11(b) that  $\epsilon_{22}^p$  behaves as  $\ln r$  as the crack tip is approached.

Logarithmic strain singularities for dynamic crack propagation in elastic-perfectly plastic solids were also reported for mode III (see, for example, SLEPYAN, 1976) and mode I plane strain (GAO and NEMAT-NASSER, 1983; GAO, 1985). It is noted here

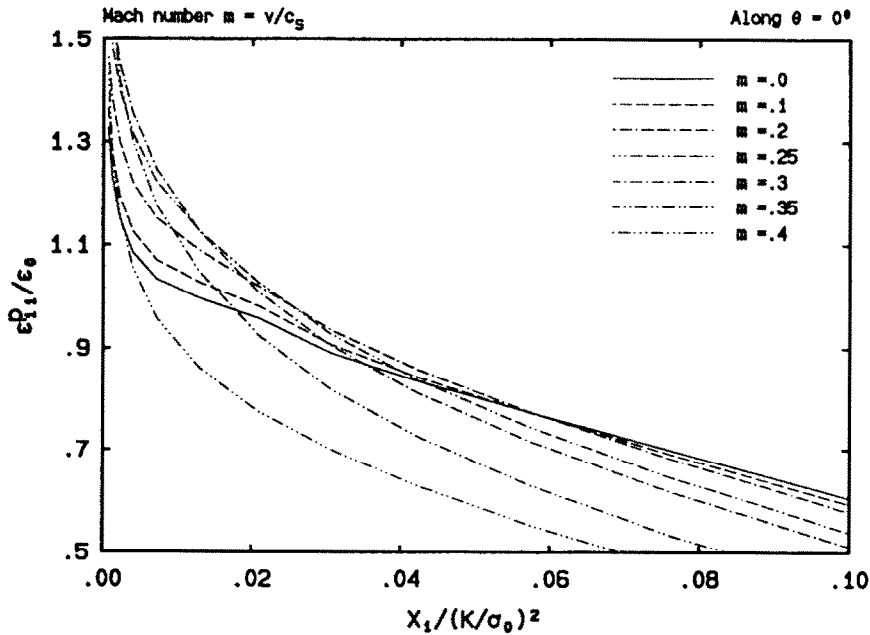


FIG. 10. The radial dependence of the 1-1 plastic strain components at crack front for various normalized crack speeds.

that in the incompressible plane strain case, a proof is offered by LEIGHTON *et al.* (1987) stating that stress discontinuities are not permissible if the maximum plastic work principle is to be satisfied, and hence they showed that  $\ln r$  type velocity or strain singularities are not permitted for this special case. GAO (1987) in his mode I plane stress asymptotic solution, assumed  $\ln r$  strain singularity, and consequently the same velocity singularity.

Since the plastic strains are dominated near the crack tip by the 2-2 component, it is expected that the effective plastic strain behaves just like the 2-2 component near the tip. Figure 12(a,b) verifies this. Here we would like to point out that since  $\epsilon_0^p$  is a measure of plastic straining, a conclusion can then be drawn from Fig. 12(a), namely that as crack speed increases, plastic straining at the crack front becomes less severe. This reduced plastic straining phenomenon in fact has been found in all three fracture modes from stationary cracks to extending cracks (for example, see DENG, 1990). Thus, at a certain fixed load-level characterized by the value of the far-field stress intensity factor  $K$ , the level of plastic straining represented by the effective plastic strain is lower for higher crack propagation speeds at the same location ahead of the crack tip. In order for the level of plastic straining at a higher crack speed to be the same as that at a lower crack speed, the loading level for the former must be raised. We will discuss this observation in more detail in Section 4, where fracture criteria are investigated.

The radial distributions of the Cartesian velocity components are presented in Fig.

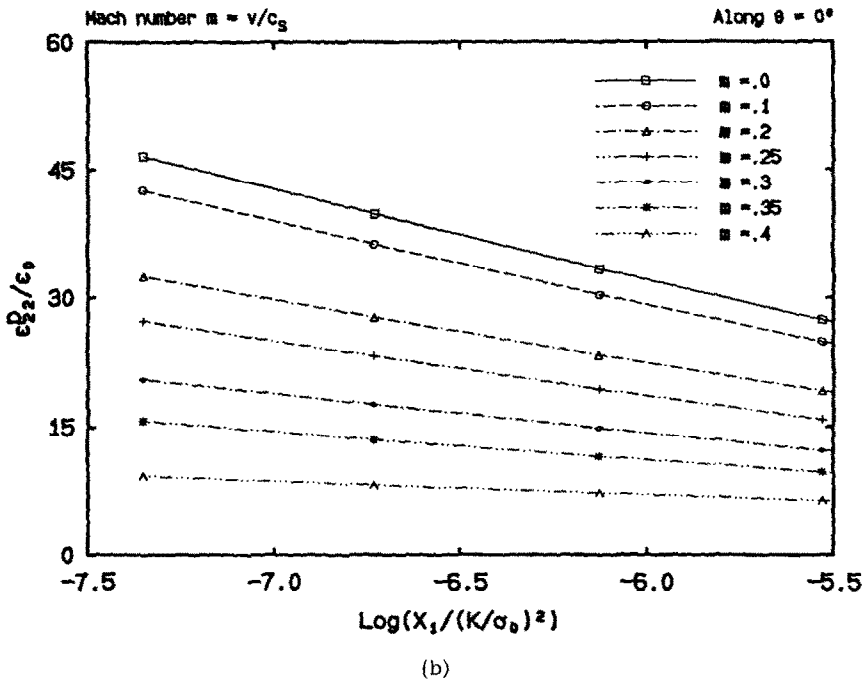
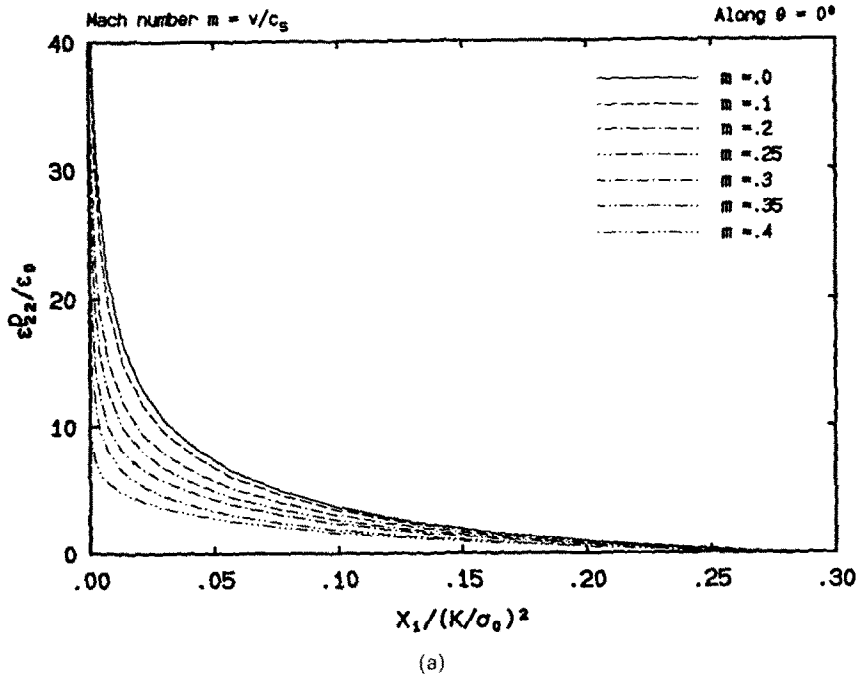
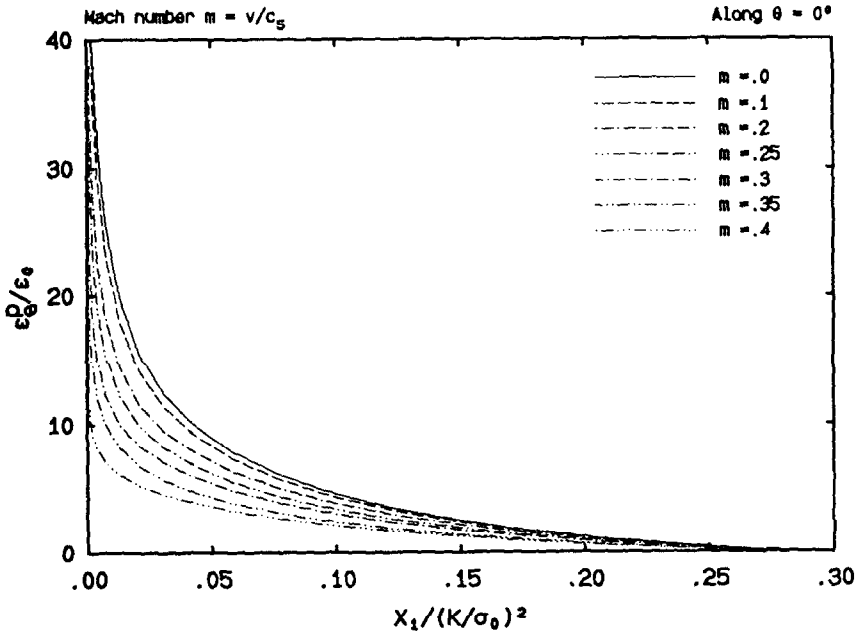
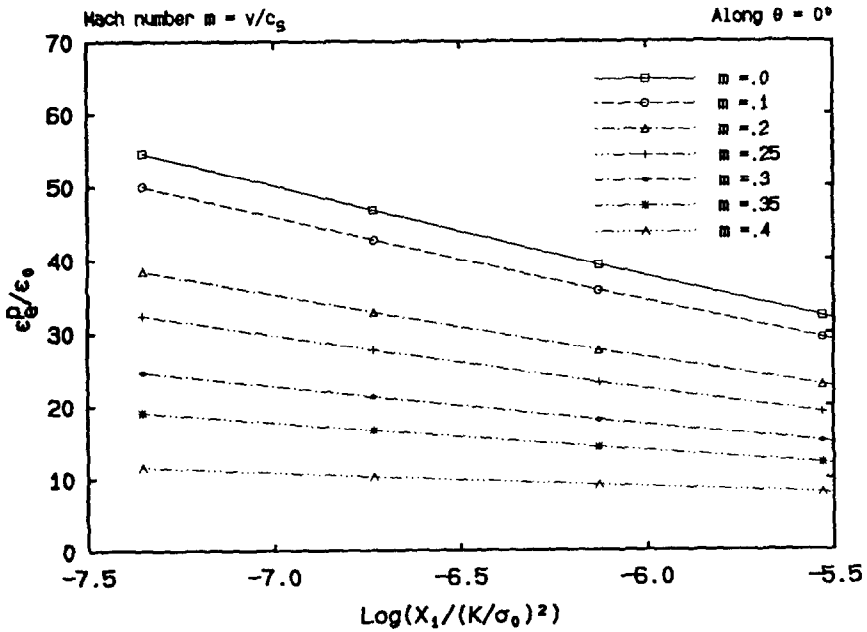


FIG. 11. (a) The radial dependence of the 2-2 plastic strain components at crack front for various normalized crack speeds. (b) The radial dependence of the 2-2 plastic strain components at crack front for various normalized crack speeds, plotted against the logarithmic values of the normalized distance.



(a)



(b)

FIG. 12. (a) The radial dependence of the effective plastic strain at crack front for various normalized crack speeds. (b) The radial dependence of the effective plastic strain at crack front for various normalized crack speeds, plotted against the logarithmic values of the normalized distance.

13 for  $v_2$  and in Fig. 14 for  $v_1$ , which are of more interest in the sense that asymptotic solutions are usually obtained in terms of velocities instead of strains. Note that the normalized velocities are plotted against the logarithmic values of the normalized distance, along two radial lines, namely along  $\theta = 45^\circ$  and  $135^\circ$ . It is discovered that while  $v_2$  behaves, especially for lower  $m$  values, as  $\ln r$  at the crack tip, the magnitude of its coefficient becomes much smaller for higher  $m$  values. Yet, interestingly enough, the opposite is observed for  $v_1$ . For small  $m$  values, approximately horizontal lines are observed, which indicates very weak or no  $\ln r$  dependence, whereas as  $m$  increases, the linear curves are found to increase their slopes significantly, which indicates strong  $\ln r$  dependence.

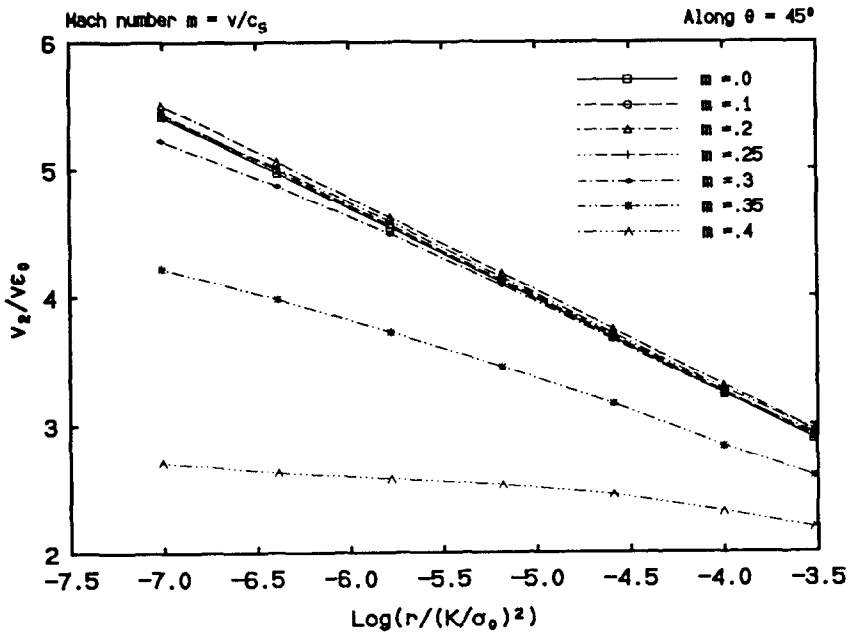
Also of some interest is the radial variation of the velocity field along the crack flank, which is shown in Fig. 15. It is seen that the magnitude of  $v_2$  decreases rapidly as the distance from the crack tip increases, but it is not clear from our results if  $v_2$  will tend to zero as the distance continue to increase. The  $v_1$  component is found to equal approximately zero at all distances from the tip.

The  $\ln r$ -velocity singularities indicated by the above finite element results and the changes of their magnitudes with respect to the crack propagation speed will be further discussed in the subsection of asymptotic analysis. At the same time, it is worth pointing out that the asymptotic analysis given by GAO (1987) assumed, to start with, that the strain field has a  $\ln r$  singularity. Hence, he essentially assumed a velocity field with a  $\ln r$  singularity. Moreover, from the form of the velocity field used, it can be derived that only the velocity component  $v_1(r, \theta)$  will have the assumed  $\ln r$  singularity, whereas the velocity component  $v_2(r, \theta)$  is bounded in Gao's solution. This feature seems contradictory to our numerical findings, which will be explained later in an asymptotic analysis.

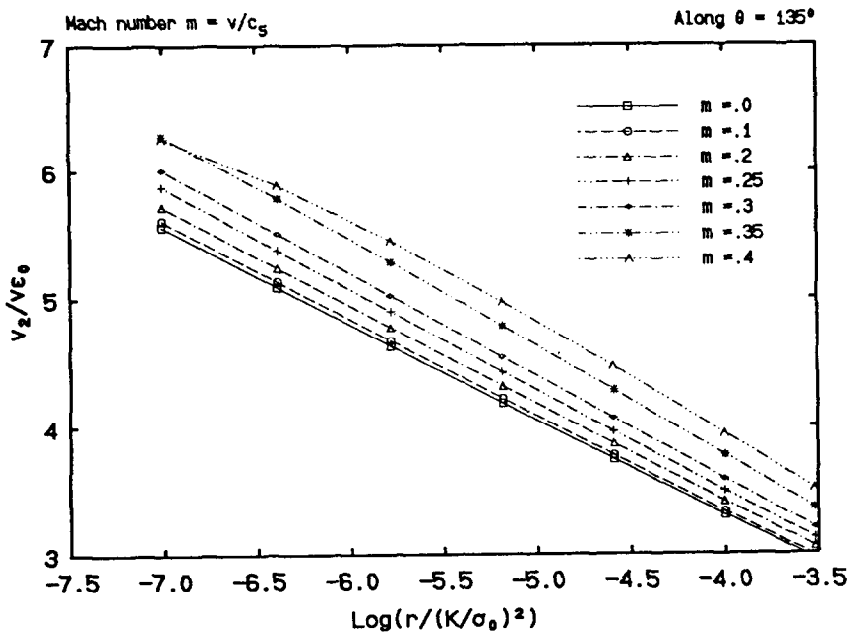
Finally we present the results for the crack surface profiles during crack propagation. The global view of the vertical displacement component  $u_2$ , which is half the crack opening displacement, is illustrated in Fig. 16(a) for different crack speeds. It is noted here that in the normalized coordinates, the magnitude of  $u_2$  increases as  $m$  increases.

The question at this point is whether this tendency will reverse, that is, how small  $r$  should be in order to see a decrease in the magnitude of  $u_2$  for increasing  $m$ . In a similar numerical study for mode I plane strain crack propagation by LAM and FREUND (1985), it is reported that for  $m$  values from 0.0 to 0.4, the reversing point is at  $r = 0.05(K/\sigma_0)^2$  behind the crack tip. However for the plane stress case, we did not find such an early reversing point. As depicted in Fig. 16(b), no reversing tendency is detected even on a length scale about one-hundredth smaller than that used by Lam and Freund, except for  $m = 0.4$  where a small deviation is noticed.

Now let us pay attention to the slope changes of the crack tip openings for different  $m$  values. From Fig. 16(b), it can be seen that while for small  $m$  values the opening profiles bend down near the crack tip, they are approximately straight lines for higher  $m$  values, whose slopes are actually rather insensitive to the crack speeds. Similar numerical results are also reported for the mode III case (DOUGLAS *et al.*, 1981). This seems to indicate a tendency that the crack opening displacement assumes asymptotically at the tip a linear radial dependence as the crack speed becomes higher, or as the dynamic effect grows larger.

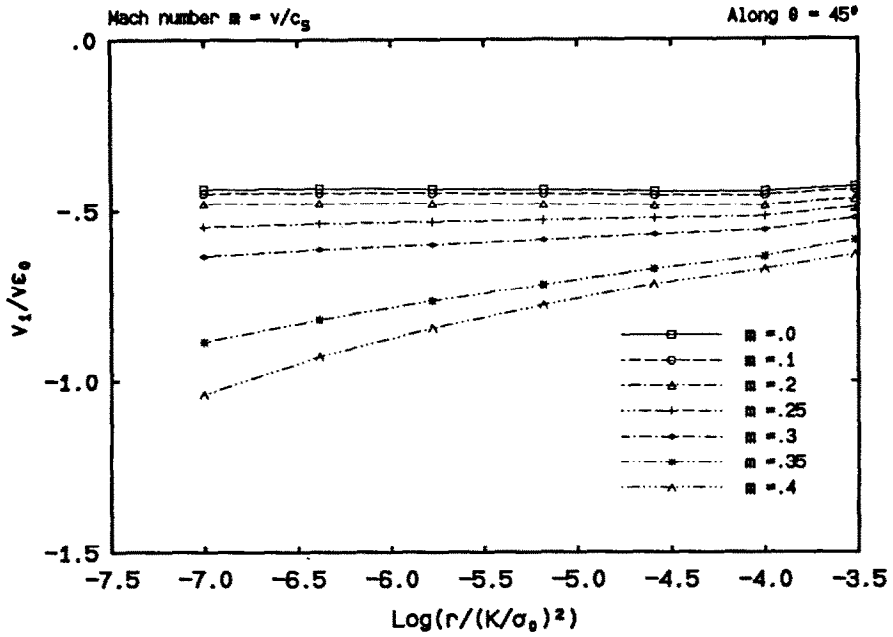


(a)

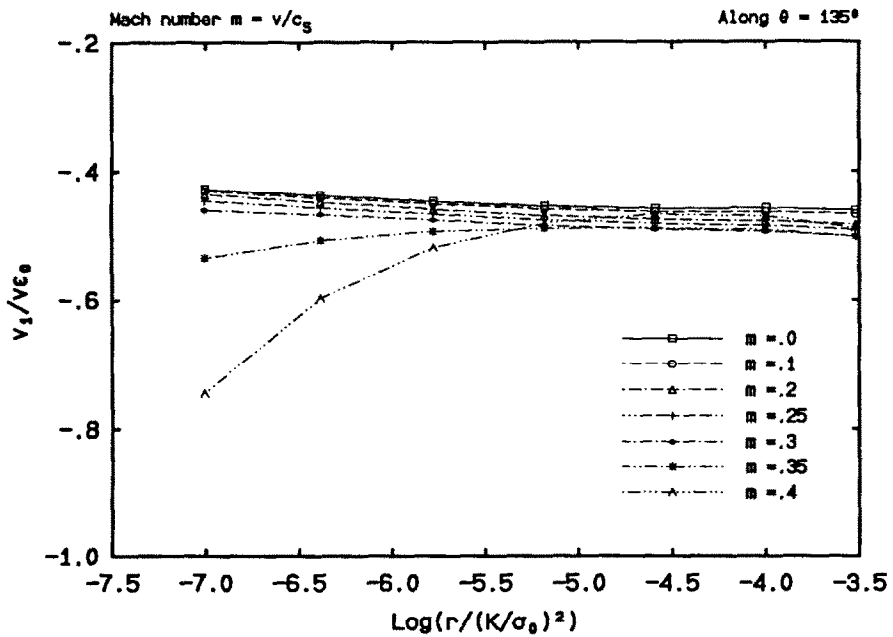


(b)

FIG. 13. (a) The radial dependence of  $v_2$  in normalized form plotted against  $\log(r/(K/\sigma_0)^2)$  along  $\theta = 45^\circ$  for various normalized crack speeds. (b) The radial dependence of  $v_2$  in normalized form plotted against  $\log(r/(K/\sigma_0)^2)$  along  $\theta = 135^\circ$  for various normalized crack speeds.



(a)



(b)

FIG. 14. (a) The radial dependence of  $v_1$  in normalized form plotted against  $\log(r/(K/\sigma_0)^2)$  along  $\theta = 45^\circ$  for various normalized crack speeds. (b) The radial dependence of  $v_1$  in normalized form plotted against  $\log(r/(K/\sigma_0)^2)$  along  $\theta = 135^\circ$  for various normalized crack speeds.

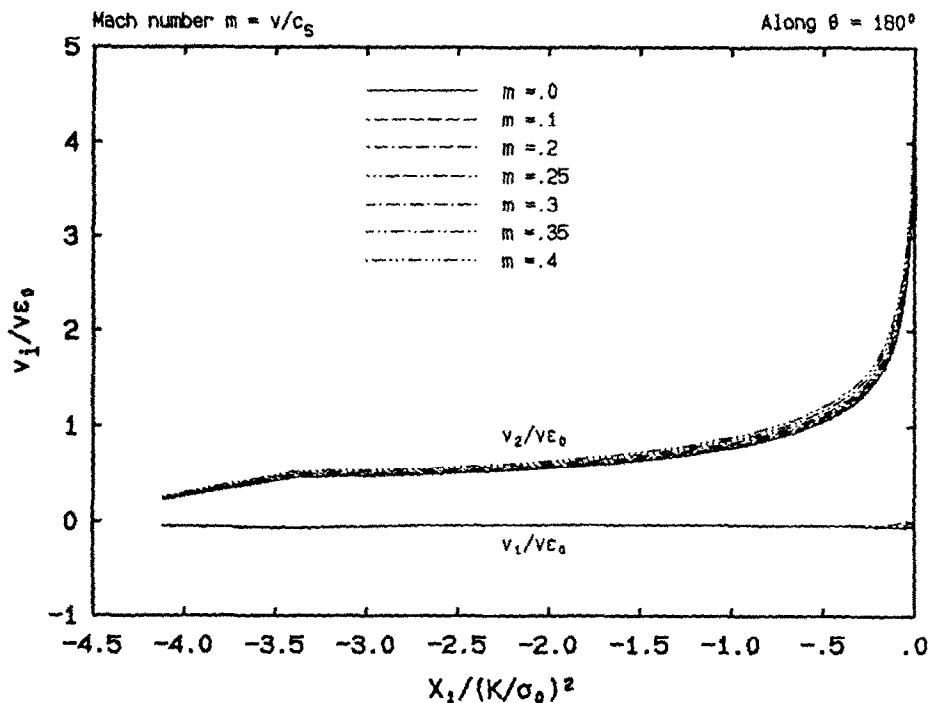


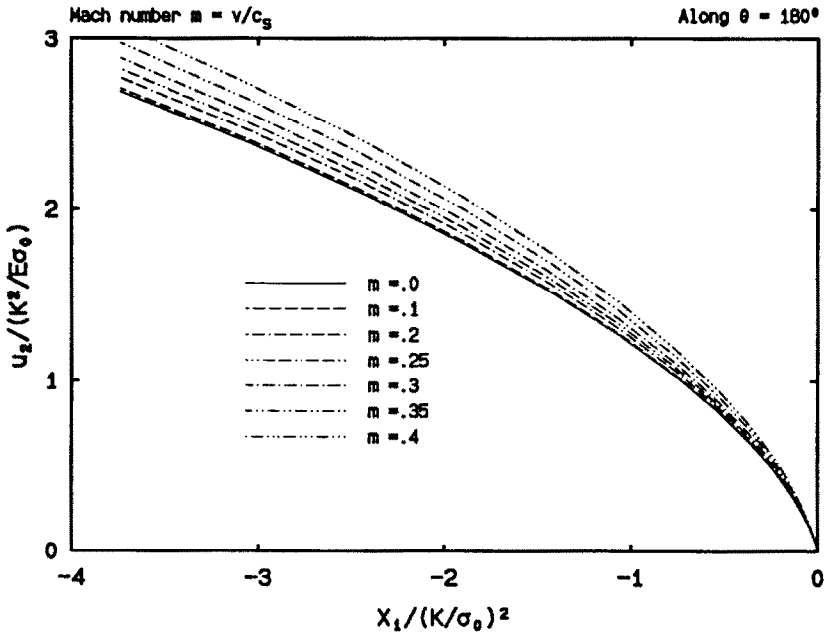
FIG. 15. The radial dependence of the velocity components along the crack flank for various normalized crack speeds.

### Asymptotic analysis

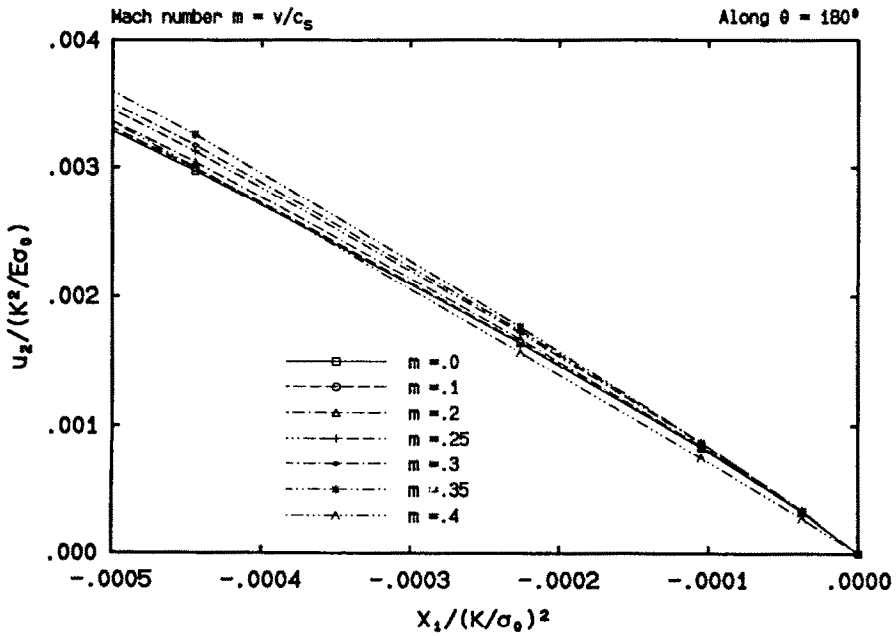
In the above we presented the results pertaining to the nature of crack tip stress and deformation fields for dynamic crack propagation in elastic perfectly plastic solids under conditions of mode I plane stress, steady state and small-scale yielding. Detailed comparisons with the asymptotic solution by GAO (1987) were performed.

It was observed that the asymptotic near-tip field by Gao involves many characteristic behaviors often contradictory to the findings of the present full field numerical study. It is noted that in Gao's analysis it is directly assumed that the strain field, and hence the velocity field possess  $\ln r$ -singularities at the crack tip, and that the stresses are bounded and can be treated as functions of  $\theta$  only. The result of the present finite element solution very near the crack tip seems to confirm the logarithmic behavior of the strain and velocity fields. However, the particular form adopted for the velocity field in Gao's asymptotic analysis implies that only the velocity component  $v_1(r, \theta)$  has a  $\ln r$ -singularity at the crack tip or  $r = 0$ , whereas the velocity component  $v_2(r, \theta)$  is bounded, which seems contrary to our numerical result.

It is our purpose here to discuss a preliminary asymptotic analysis regarding the near-tip radial dependence of the velocity field and of the crack opening displacement.



(a)



(b)

FIG. 16. (a) The radial dependence of the displacement component  $u_2$  along the crack flank for various normalized crack speeds. (b) A detailed view of the radial dependence of the displacement component  $u_2$  along the crack flank for various normalized crack speeds.

Certain features of the numerically determined crack tip field and their differences with Gao's asymptotic solution will be interpreted accordingly. No direct assumptions about the singularity of the velocity field and the boundedness of the stress field will be made, although assumptions of other types are still necessary.

Now suppose a crack is propagating steadily (see Fig. 1) under mode I plane stress conditions in an elastic-perfectly plastic solid obeying the von Mises yield criterion and the associated flow rule. From the steady-state condition, it is necessary that the crack tip velocity  $v$  be a constant and that for any field quantity, say  $q$ , its material time derivative be computed from (2.1). For an actively yielded stress state  $\sigma_{ij}$ , the yield condition requires that

$$s_{ij}s_{ij} = \tau_0^2, \quad (3.1a)$$

where  $\tau_0$  is the yield stress in simple shear,  $s_{ij}$  is the deviatoric stress tensor component given by

$$s_{ij} = \sigma_{ij} - \frac{1}{3}\sigma_{kk}\delta_{ij}. \quad (3.1b)$$

It is understood here that Latin indices have range one to three while Greek indices have range one and two, and that the standard indicial notation and its associated conventions are used. The plane stress condition simplifies the above equations with

$$\sigma_{3i} = 0. \quad (3.2)$$

Immediately from (3.1a), it is seen that  $s_{ij}$  must be bounded. Since  $\sigma_{33} = 0$ , then from (3.1b),  $\sigma_{kk} = -3s_{33}$ . Hence  $\sigma_{kk}$  is also bounded. Consequently, it can be concluded from (3.1b) that  $\sigma_{ij}$  must be bounded.

To investigate the asymptotic structure of the crack tip field, let us consider a generic sector at the crack tip. Suppose the sector is confined by two straight radial lines from the crack tip. We further assume that all limits taken below exist in this sector such that operations on the order symbols are permissible within this sector.

Next define  $\bar{\sigma}_{ij}(\theta)$ , a function of  $\theta$  at the crack tip, as follows

$$\bar{\sigma}_{ij}(\theta) = \lim_{r \rightarrow 0} \sigma_{ij}(r, \theta), \quad (3.3a)$$

and let

$$\hat{\sigma}_{ij}(r, \theta) = \sigma_{ij}(r, \theta) - \bar{\sigma}_{ij}(\theta). \quad (3.3b)$$

Then the stress state  $\sigma_{ij}(r, \theta)$  near the crack tip can be expressed as

$$\sigma_{ij}(r, \theta) = \bar{\sigma}_{ij}(\theta) + \hat{\sigma}_{ij}(r, \theta). \quad (3.3c)$$

Hence from (3.3a) and (3.3b), it is true that  $\lim_{r \rightarrow 0} \hat{\sigma}_{ij}(r, \theta) = 0$ , or that, using the order symbols (see, for example, ERDÉLYI, 1956),  $\hat{\sigma}_{ij}(r, \theta) = o(1)$  as  $r \rightarrow 0$ . Then we must have  $\partial \hat{\sigma}_{ij} / \partial r = o(1/r)$  as  $r \rightarrow 0$ , since otherwise if  $\partial \hat{\sigma}_{ij} / \partial r = O(1/r)$  as  $r \rightarrow 0$ , we would have  $\hat{\sigma}_{ij}(r, \theta) = O(\ln r)$  as  $r \rightarrow 0$ , which violates our original conclusion.

Now it is established that  $\partial \hat{\sigma}_{ij} / \partial r = o(1/r)$  as  $r \rightarrow 0$ , then  $r(\partial \hat{\sigma}_{ij} / \partial r) = o(1)$  as  $r \rightarrow 0$  or  $\lim_{r \rightarrow 0} r(\partial \hat{\sigma}_{ij} / \partial r) = 0$ . Hence from (3.3c),  $\lim_{r \rightarrow 0} r(\partial \sigma_{ij} / \partial r) = 0$ . Using the above

results and the following identities

$$\frac{\partial(\ )}{\partial x_1} = \cos \theta \frac{\partial(\ )}{\partial r} - \frac{\sin \theta}{r} \frac{\partial(\ )}{\partial \theta}, \quad (3.4a)$$

$$\frac{\partial(\ )}{\partial x_2} = \sin \theta \frac{\partial(\ )}{\partial r} + \frac{\cos \theta}{r} \frac{\partial(\ )}{\partial \theta}, \quad (3.4b)$$

it can be proved that

$$\frac{\partial \sigma_{ij}}{\partial x_\alpha} = O\left(\frac{1}{r}\right) \quad (\alpha = 1, 2) \quad \text{as } r \rightarrow 0. \quad (3.5)$$

In order to investigate the singularity of the velocity field  $v_\alpha(r, \theta)$  at the crack tip, a study of the basic equations is necessary. Under steady state and plane stress conditions, the equation of motion in the crack tip moving coordinate system will be

$$\frac{\partial \sigma_{\alpha\beta}}{\partial x_\beta} = -v\rho \frac{\partial v_\alpha}{\partial x_1}, \quad (3.6)$$

where  $v$  is the crack propagation speed and  $\rho$  is the mass density of the material. Similarly, the constitutive law can be written as

$$\frac{\partial v_1}{\partial x_1} = -\frac{v}{E} \left[ (1+\nu) \frac{\partial \sigma_{11}}{\partial x_1} - \nu \frac{\partial \sigma_{kk}}{\partial x_1} \right] + \frac{\dot{\lambda}}{3} (2\sigma_{11} - \sigma_{22}), \quad (3.7a)$$

$$\frac{\partial v_2}{\partial x_2} = -\frac{v}{E} \left[ (1+\nu) \frac{\partial \sigma_{22}}{\partial x_1} - \nu \frac{\partial \sigma_{kk}}{\partial x_1} \right] + \frac{\dot{\lambda}}{3} (2\sigma_{22} - \sigma_{11}), \quad (3.7b)$$

$$\frac{\partial v_1}{\partial x_2} + \frac{\partial v_2}{\partial x_1} = -\frac{2v(1+\nu)}{E} \frac{\partial \sigma_{12}}{\partial x_1} + 2\dot{\lambda}\sigma_{12}, \quad (3.7c)$$

where  $E$  is the Young's modulus,  $\nu$  is the Poisson ratio, and  $\dot{\lambda}$  is the plastic flow factor such that it is zero for an elastic stress state and it is nonnegative for an actively yielded stress state.

From (3.5) and (3.6) it is clear that

$$\frac{\partial v_\alpha}{\partial x_1} = O\left(\frac{1}{r}\right) \quad \text{as } r \rightarrow 0. \quad (3.8a)$$

It is our purpose here to show that

$$\frac{\partial v_\alpha}{\partial x_2} = O\left(\frac{1}{r}\right) \quad \text{as } r \rightarrow 0, \quad (3.8b)$$

for all elastic sectors and for plastic sectors where  $\sigma_{22} \neq 2\sigma_{11}$ .

First of all, for a sector in an elastic stress state,  $\dot{\lambda} = 0$ . Then, noting (3.5) and (3.8a), it is clear from (3.7b) and (3.7c) that (3.8b) holds.

Secondly, in a plastic sector where  $\sigma_{22} \neq 2\sigma_{11}$ , it can be shown from (3.5), (3.7a) and (3.8a) that  $\dot{\lambda} = O(1/r)$  as  $r$  approaches zero. Substitution of  $\dot{\lambda}$  into (3.7b) and (3.7c) will then readily yield (3.8b).

In fact, the results of the present finite element study seem to suggest that the crack tip is surrounded completely by these two types of sectors, as shown in Fig. 17. Nevertheless, if both (3.8a) and (3.8b) hold, then from the chain rule  $\partial v_x/\partial r = (\partial v_x/\partial x_\beta)(\partial x_\beta/\partial r)$  and the identities  $\partial x_1/\partial r = \cos \theta$  and  $\partial x_2/\partial r = \sin \theta$ , it can be concluded that

$$\frac{\partial v_x}{\partial r} = O\left(\frac{1}{r}\right) \text{ as } r \rightarrow 0. \tag{3.9}$$

Consequently,  $v_x = O(\ln r)$  as  $r \rightarrow 0$ . Without loss of generality,  $v_x$  can then be written as

$$v_x(r, \theta) = g_x(\theta) \ln r + f_x(r, \theta) + h_x(\theta) + o(1), \text{ as } r \rightarrow 0, \tag{3.10}$$

where  $g_x$  and  $h_x$  are bounded functions of  $\theta$ , and  $f_x$  is singular at  $r = 0$  yet less singular than  $\ln r$ .

It is claimed here that  $g_x$  must be a constant and that  $f_x$  must be a function of  $r$  only. This is true since otherwise from (3.10) and (3.4) we would have

$$\frac{\partial v_x}{\partial x_1} = -\sin \theta \frac{\partial g_x}{\partial \theta} \frac{\ln r}{r} - \sin \theta \frac{\partial f_x}{\partial \theta} \frac{1}{r} + O\left(\frac{1}{r}\right), \tag{3.11a}$$

$$\frac{\partial v_x}{\partial x_2} = \cos \theta \frac{\partial g_x}{\partial \theta} \frac{\ln r}{r} + \cos \theta \frac{\partial f_x}{\partial \theta} \frac{1}{r} + O\left(\frac{1}{r}\right), \tag{3.11b}$$

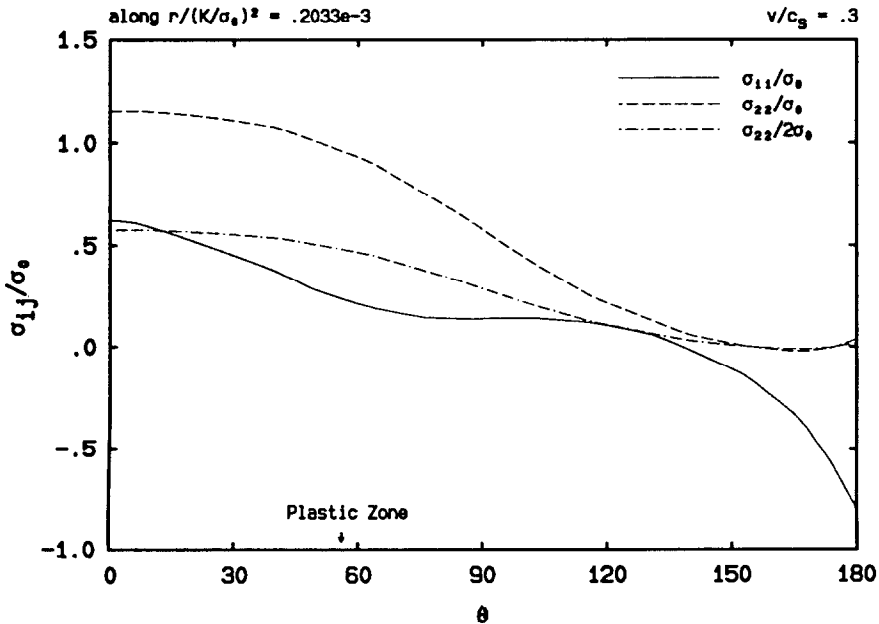


FIG. 17. Angular variations of  $\sigma_{11}$ ,  $\sigma_{22}$  and  $\sigma_{22}/2$  for  $v/c_0 = 0.3$ , normalized by  $\sigma_0$ .

as  $r$  approaches zero. Note that  $\partial g_\alpha(\theta)/\partial\theta \neq 0$  and that  $\partial f_\alpha(r, \theta)/\partial\theta$  is singular at  $r = 0$ . Hence (3.11) would mean that  $\partial v_\alpha/\partial x_\beta$  is more singular than  $1/r$  as  $r \rightarrow 0$ , which contradicts (3.8).

At the moment we have shown that if the limits as  $r \rightarrow 0$  taken in the above deductions exist, if operations on the order symbols are permissible, and if the crack tip is only composed of, as indicated by the results of the present finite element analysis, elastic sectors and those plastic sectors within which  $\sigma_{22} \neq 2\sigma_{11}$ , then the velocity field can be expressed as

$$v_\alpha(r, \theta) = c_\alpha \ln r + f_\alpha(r) + h_\alpha(\theta) + O(1), \quad \text{as } r \rightarrow 0, \quad (3.12)$$

where the coefficients  $c_1$  and  $c_2$  are constants. Further, if velocity continuity is enforced, both  $c_2$  and  $f_2$  would be identically zero as required by the symmetry condition  $v_2 = 0$  at  $\theta = 0$ .

The velocity field expressed in (3.12) with  $c_2 = 0$  and  $f_\alpha$  excluded is the one essentially assumed in Gao's asymptotic analysis. On the other hand, our finite element results reveal that the velocity component  $v_2$  possesses  $\ln r$ -singularity, which is apparent from Fig. 13 at least for  $v/c_s \leq 0.35$ . An inconsistency seems to exist. To this end, the following explanation is suggested.

First note that in Fig. 13, there are indeed signs that the  $\ln r$ -singularity of the velocity component  $v_2$  is dying out as  $m$  or  $v/c_s$  increases, as evidenced by the tendency of the declining magnitude of slope of the straight lines in Fig. 13. Secondly, discoveries from mode III dynamic crack growth have demonstrated that the dominance zone of a first-order dynamic asymptotic solution is very small such that it vanishes rapidly as  $v/c_s$  decreases. In other words, characteristics of the leading asymptotic behavior of the crack tip fields can be clearly detected for a certain finite element mesh only at a sufficiently large crack propagation speed. This would mean that the numerical results for  $v/c_s \leq 0.35$  (and for  $r \geq 0.2033 \times 10^{-3} (K/\sigma_0)^2$ ) are essentially the solution for quasi-static crack growth or a mixture of both quasi-static and dynamic fields.

Moreover, if (3.12) is taken to be valid and  $c_2$  and  $f_2$  are set to zero in order to satisfy the symmetry conditions at  $\theta = 0^\circ$ , then the crack opening displacement (which is twice the vertical displacement  $u_2$  at  $\theta = 180^\circ$ ), which can be obtained by integrating  $v_2$  with respect to  $r$  along  $\theta = 180^\circ$ , would be linearly dependent on  $r$  or the radial distance to the crack tip. This linear behavior indeed seems to exist for crack propagation speed higher than a certain value (e.g. the curve for  $m = 0.4$  in Fig. 16b).

Recall that for crack propagation at low speeds, no plastic reloading has been detected along the crack flank (see Fig. 4). At the same time, it is noticed that the slope of the straight lines in Fig. 14(a) or the coefficient for the  $\ln r$  singularity of the velocity component  $v_1$  is approximately zero for small  $m$  values. To explain this behavior, it will be demonstrated in the following that the elastic (unloading) sector behind the crack front plastic sectors must be ended (near  $\theta = 180^\circ$ ) with a trailing plastic sector, or otherwise, the coefficient for the  $\ln r$ -term, in  $v_1$  must be zero.

In fact, suppose the elastic unloading sector extends all the way down to the crack surface. Then, since it is in an elastic sector, (3.7a) becomes

$$\frac{\partial v_1}{\partial x_1} = -\frac{v}{E} \left[ (1+v) \frac{\partial \sigma_{11}}{\partial x_1} - v \frac{\partial \sigma_{kk}}{\partial x_1} \right], \quad (3.13)$$

which can be integrated with respect to  $x_1$  to yield

$$-\frac{v}{E}[(1+v)\sigma_{11} - v\sigma_{kk}] = v_1 + P(x_2), \quad (3.14)$$

where  $P(x_2)$  is a function of  $x_2$  resulting from the integration.

Now from (3.12)  $v_1(r, \theta) = c_1 \ln r + O(1)$  as  $r \rightarrow 0$ . Since it has been shown that the stresses must be bounded, then from (3.14), the quantity  $c_1 \ln r + P(x_2)$  must be bounded. Thus in order to cancel the nonboundedness of this quantity at  $r = 0$  due to the  $\ln r$  singularity, the function  $P(x_2)$  must be such that

$$P(x_2) = -c_1 \ln |x_2| + \hat{P}(x_2) = -c_1 \ln r - c_1 \ln |\sin \theta| + \hat{P}(x_2),$$

where  $\hat{P}(x_2)$  is bounded. Hence, the quantity  $-c_1 \ln |\sin \theta| + \hat{P}(x_2)$  or  $c_1 \ln |\sin \theta|$  must be bounded since by definition  $\hat{P}(x_2)$  is already bounded. This will necessarily require that  $c_1 = 0$  since otherwise the whole term will not be bounded due to the fact that  $\ln |\sin \theta| \rightarrow \infty$  as  $\theta \rightarrow 180^\circ$ . This proves the previous claim.

#### 4. FRACTURE CRITERIA

There are many issues regarding the use of  $K$  as a fracture characterizing parameter for dynamic crack propagation, not only due to experimental discrepancies, as discussed in the introductory section, but also due to the fact that  $K$ , even under small-scale yielding conditions, no longer retains its many fine properties as in the case of fracture initiation. Because of the existence of the residual plastic wake behind the crack tip,  $K$ , in the case of crack growth, loses its simple relationship with the energy release rate  $G$ , which is somehow the physical ground for postulating the  $K$ -criterion for fracture initiation. Also because of the existence of the plastic wake, the singular  $K$ -field does not completely surround the crack tip elastic-plastic zone, and it is not clear whether  $K$  still characterizes the fracture behavior at the crack tip. To summarize, directly assuming the validity of the  $K$ -criterion for dynamic crack propagation in elastic-plastic materials has no solid theoretical grounds. However, as we know, there has been vast time-investment in developing and standardizing  $K$ -measurement techniques and instruments, and well-documented data are widely available. It is therefore of vital importance to carefully investigate the validity of the  $K$ -criterion from a more fundamental point of view, and to properly assess its accuracy and reliability as a practical fracture criterion.

It is our purpose in this section to demonstrate, instead of directly assuming, the legitimacy of the  $K$ -criterion for dynamic crack propagation in solids which fail in a locally ductile manner through the use of more fundamental fracture criteria such as those directly based on the near-tip deformation field. In particular, we will utilize the McClintock-Irwin critical plastic strain criterion (McCLINTOCK and IRWIN, 1964) to extract theoretical  $K_{Ic}^d$  vs  $v$  curves from our numerical full field solutions for mode I plane stress crack tip fields in elastic-perfectly plastic solids, where  $K_{Ic}^d$  is the critical dynamic stress intensity factor in plane stress, and  $v$  is the speed of crack propagation. Good agreement with experimental results on 4340 steel will be demonstrated. We will also point out the source of difficulty, or impossibility to be more accurate in

some circumstances, to extract such a  $K_{Ic}^d$  vs  $v$  relation from a crack tip opening displacement-based fracture criterion. Theoretical implications of this phenomenon will be addressed.

As is well known, fracture criteria based on the energy release rate  $G$  (IRWIN, 1956), the stress intensity  $K$ , and the  $J$ -integral (RICE, 1968) have clear physical meanings and sound theoretical bases when used for the onset of crack growth in elastic-plastic solids under proper constraints, or when used for continued crack growth in ideally brittle solids. Under elastic-plastic stable crack growth conditions, however, these criteria themselves cannot tell the sources of increased material resistance to continued fracture. Hence, it is impossible to utilize them to generate theoretical material resistance curves (ASTM STP 527, 1974) without invoking more fundamental assumptions, such as those based on plastic strains at crack front, or those based on the crack opening displacement behind the crack tip. Besides, they cannot be extended without more fundamental studies to cases beyond their limits, such as cases involving dynamic crack propagation.

Fracture criteria based on the crack opening displacement are frequently used in plane strain, where plastic straining is not most severe directly at the crack front (see, for example, a review by DENG, 1990). One such criterion is proposed by RICE and SORENSEN (1978), which assumes that fracture initiation and continued crack growth can occur if a critical crack tip opening  $\delta_c$  is maintained at a small characteristic distance  $r_m$  behind the tip. This criterion can be viewed as a critical crack opening angle criterion, and has been used successfully, under plane strain conditions, to explain the phenomenon of increased material resistance to continued fracture for stable crack growth (RICE *et al.*, 1980).

The Rice-Sorensen critical crack tip opening angle criterion has more recently been applied to extract theoretical  $K_{Ic}^d$  vs  $v$  curves for mode I plane strain dynamic crack propagation by LAM and FREUND (1985). Under steady-state and small-scale yielding conditions, they employed the Eulerian type finite element formulation originally proposed by DEAN and HUTCHINSON (1980) for quasi-static crack extension. From crack opening results very near the crack tip, they were able to generate the crack-speed dependence of the critical dynamic stress intensity factor, which are qualitatively very similar to the experimental findings of ROSAKIS *et al.* (1984).

The application of this criterion to our mode I plane stress case is however not successful. Data for the critical dynamic stress intensity, or the dynamic fracture toughness  $K_{Ic}^d$ , obtained from laboratory tests performed on thin metal plates, which fracture in a locally ductile manner, exhibit a monotonic rising tendency as the crack speed  $v$  increases (see, e.g., ROSAKIS *et al.*, 1984; ZEHNDER and ROSAKIS, 1990). In order to predict such a tendency with the Rice-Sorensen criterion, it is necessary for the so-defined crack tip opening angle  $\delta(r)/r$ , when plotted against the normalized toughness value  $K_{Ic}^d/K_{ss}$  with  $K_{ss}$  being the quasi-static steady-state value, to have lower values for higher crack speeds when the normalized toughness is fixed. Another requirement is that when the same plot is used, the quantity  $K_{Ic}^d/K_{ss}$  should have lower values for lower crack speeds when the opening angle is fixed. We notice that such a tendency is indeed observed for mode I plane strain (see Fig. 6 of the paper by LAM and FREUND, 1985). Yet this is not the case in mode I plane stress for elastic-perfectly plastic materials, although our finite element mesh is much finer than that employed

by Lam and Freund. In fact, we did not observe such a tendency even on a scale about one-hundredth finer than that of the previous two authors. The same situation is also reported by DOUGLAS *et al.* (1981) for mode III.

The difficulty in applying critical crack tip opening angle criterion to mode III and mode I plane stress can in one way be attributed to numerical errors accumulated near the crack tip. One such error is simply due to the lack of enough spatial resolution near the crack tip. This leads to the usual finite element discretization error which alone would blur the real behavior of the crack tip opening profile. To this end, it is emphasized here that the mesh we employed has a ratio of plastic zone size to the smallest element size on the order of  $1.6 \times 10^4$ , which is already a very high resolution. Another source of numerical error is somewhat peculiar to the Eulerian formulation in which updated stresses are obtained through numerical integrations of the incremental constitutive law from crack front to crack back. This integration, after sweeping the crack tip, carries large discretization errors to the areas behind the crack tip, which is most significant immediately near the tip. The crack tip opening profile, which is to be used in a fracture criterion, happens to be most inaccurate there.

Another factor contributing to this difficulty may come from the asymptotic nature of the crack tip fields in mode I plane stress and in mode III. Taking the mode III case as an example, the asymptotic solution for dynamic crack propagation by SLEPYAN (1976) predicts a crack tip opening as

$$\delta(r) = 2u_3|_{\theta=\pi} = \frac{\pi\tau_0}{\mu m} r,$$

where  $\tau_0$  is the initial yield stress in shear,  $\mu$  is the elastic shear modulus. The above relation, although it gives the desired property that  $\delta(r)/r$  decreases as the normalized crack speed  $m$  increases, was not confirmed by the full field numerical solution of DOUGLAS *et al.* (1981). To this end, we would like to recall the discovery of FREUND and DOUGLAS (1982) that the region of dominance of the dynamic asymptotic solution vanishes as the crack speed goes to zero. In light of this, it is very possible that the region in which the desired property of the crack opening displacement exists in order to apply the critical angle criterion is vanishingly small such that no numerical study of reasonable cost can detect such a presence. Besides, there is a physical lower limit to the size of the region along the crack faces where the calculated crack tip opening displacement values can be used meaningfully. As pointed out by RICE *et al.* (1980), the characteristic distance  $r_m$  behind the crack tip in the Rice Sorensen criterion should be a size comparable to that of the fracture process zone ahead of the crack tip. Considering the similarities between mode III fracture and the fracture in mode I plane stress, and the fact that we have already used a very fine finite element mesh near the crack tip, it is believed that this difficulty, or impossibility, to use the critical crack opening angle criterion to extract  $K_{Ic}^d$  vs  $v$  curves is due to the asymptotic nature of the mode I dynamic plane stress crack tip fields. In fact, when the crack speed is higher, i.e. when the dominance zone of the dynamic asymptotic crack tip field is larger, the above mentioned desirable crack opening property is indeed observed (see Fig. 16b), which somehow verifies our previous belief.

The aforementioned difficulty thus leaves us only one choice, that is, to use the plastic strain-based fracture criterion, or the McClintock-Irwin critical plastic strain

criterion to be more specific. The criterion assumes that fracture occurs when the crack-front plastic strain level at a characteristic distance away from the crack tip reaches a critical value (MCCLINTOCK and IRWIN, 1964). The characteristic distance is of the order of grain or subgrain size and should be determined experimentally. In light of this, we would like to recall some consistent observations regarding the change of magnitudes of plastic strains from various solutions in the literature, which are discussed extensively in a review by DENG (1990).

It is observed by many that for stationary cracks, strains have  $1/r$  singularity at the crack tip for all three fracture modes. For advancing cracks, the singularity changes at crack front from  $\ln^2(r)$  for quasi-static crack growth to  $\ln r$  for dynamic crack propagation in mode III. In mode I plane strain for the case of Poisson ratio  $\nu = 0.5$ , plastic strains possess logarithmic singularities at least in the centered fan sector for quasi-static crack growth, yet the singularities of the strains become weaker for rapid crack extension. Thus it may be concluded that crack growth reduces the level of plastic strain concentration at the crack tip if the same remote load-level is maintained.

Likewise in mode I plane stress, as depicted in Figs 11(a) and 12(a), the magnitudes of plastic strains at the crack front decrease as the crack speed increases if the stress intensity factor is fixed at the same level. In other words, to maintain the same strain level at the same point ahead of the crack, greater stress intensity factors must be maintained for higher crack speeds, which is the behavior observed in mode I fracture for many metals. Note that since strain rate sensitivity is not considered in the above dynamic analyses, inertia alone is expected to be responsible for such behaviors.

Thus under small-scale yielding conditions, monotonically rising  $K_{Ic}^d$  vs  $v$  curves can be obtained from a full field, or simply a crack-line solution, if the critical plastic strain criterion is assumed. The first successful application of this criterion was performed by FREUND and DOUGLAS (1982) for mode III dynamic crack propagation in elastic-perfectly plastic solids. Their theoretical curves are qualitatively very similar to the findings of ROSAKIS *et al.* (1984) from experiments conducted on thin, high strength steel plates and assuming generalized plane stress conditions. From both the theoretical and practical point of view, it would then be very interesting to observe such a good correlation between theory and experiments under approximately the same type of constraints, basically the plane stress or generalized plane stress conditions.

The radial dependence of the effective plastic strain at the front of a mode I plane stress crack tip is illustrated in the usual normalized form in Fig. 18 in much detail for crack velocities ranging from 0–40% of the elastic shear wave speed of the elastic-perfectly plastic material. We note that the effective plastic strain  $\epsilon_p^e$  is normalized by  $\epsilon_0$ , the initial yield strain in tension, and that the radial distance  $X_1$  along the prospective crack line is normalized by  $(K/\sigma_0)^2$ , where  $K$  is the generic dynamic stress intensity factor and  $\sigma_0$  is the initial yield stress in tension. The procedure we used to extract the  $K_{Ic}^d$  vs  $v$  curves from numerical results is outlined as follows. First a critical plastic strain value is chosen and a horizontal line corresponding to this value is drawn on the plot, which intersects the various effective plastic strain distribution curves at different normalized radial locations. If we denote the intersection location for the quasi-static curve by  $X_1/(K_{ss}/\sigma_0)^2$ , where  $K_{ss}$  is the critical stress intensity factor for steady-state quasi-static crack growth, and denote the intersection location for a

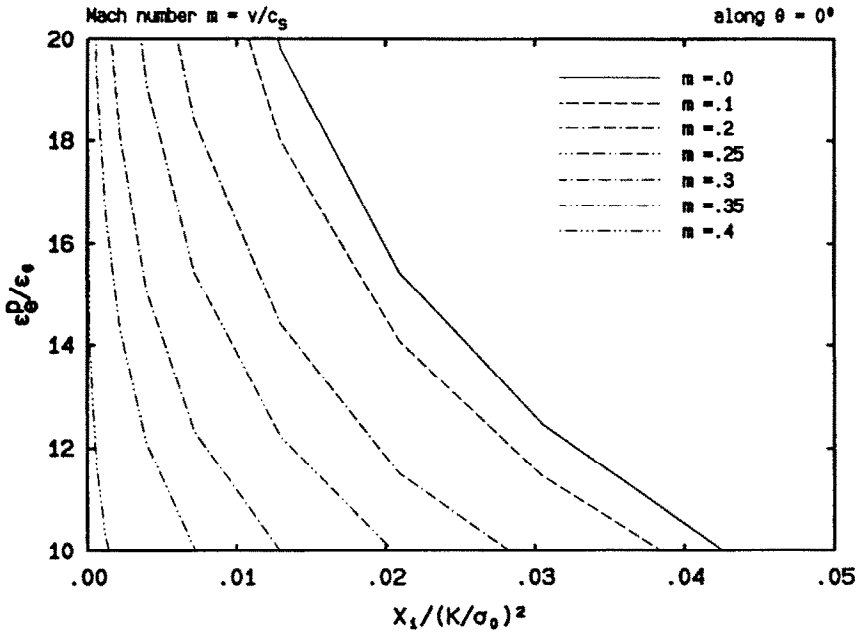


FIG. 18. The radial dependence of the effective plastic strain at the crack front along the prospective crack line.

generic  $m$  value ( $m$  being the ratio of crack tip speed to the shear wave speed) by  $X_1/(K_{lc}^d/\sigma_0)^2$ , where  $K_{lc}^d$  is the critical dynamic stress intensity factor corresponding to Mach number  $m$ , we would obtain for each  $m$  the ratio of  $(K_{lc}^d)^2$  to  $(K_{ss})^2$ , and hence the value  $K_{lc}^d/K_{ss}$ , by dividing the second location by the first, since it is assumed that the critical plastic strain value is achieved at the same physical location  $X_1$  for all  $m$ .

We would like to point out at this stage that the procedure we discussed above is different from the one employed by Freund and Douglas. Specifically, their procedure needs to use results for stationary cracks (which may not always be available), whereas ours does not. Another advantage of this procedure is that comparisons with dynamic experimental results are made easier and clearer. In fact, since all curves start at one at  $m = 0$  because of our normalization, the experimental data can be similarly normalized without relying on the availability of the fracture toughness value for the onset of crack extension.

The resultant theoretical toughness curves are shown in Fig. 19 for  $\epsilon_p^e$  ranging from  $11\epsilon_0$  to  $19\epsilon_0$ . It is found that as the value of the critical plastic strain increases, the toughness curve becomes steeper for higher  $m$  values, while at the same time the curve remains fairly flat for lower  $m$  values, where  $m$  is the ratio of the crack velocity to the shear wave speed.

Comparisons with experimental data are made in Fig. 20. Note that the results by ROSAKIS *et al.* (1984) and by ZEHNDER and ROSAKIS (1990) are obtained from

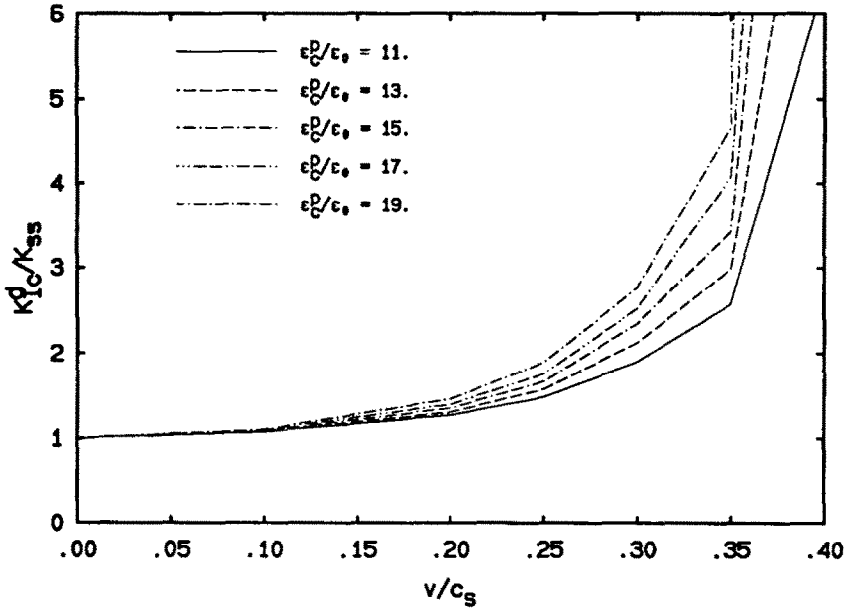


FIG. 19. Theoretical  $K_{Ic}^d$  vs  $v$  curves in their normalized forms for various critical plastic strain levels.

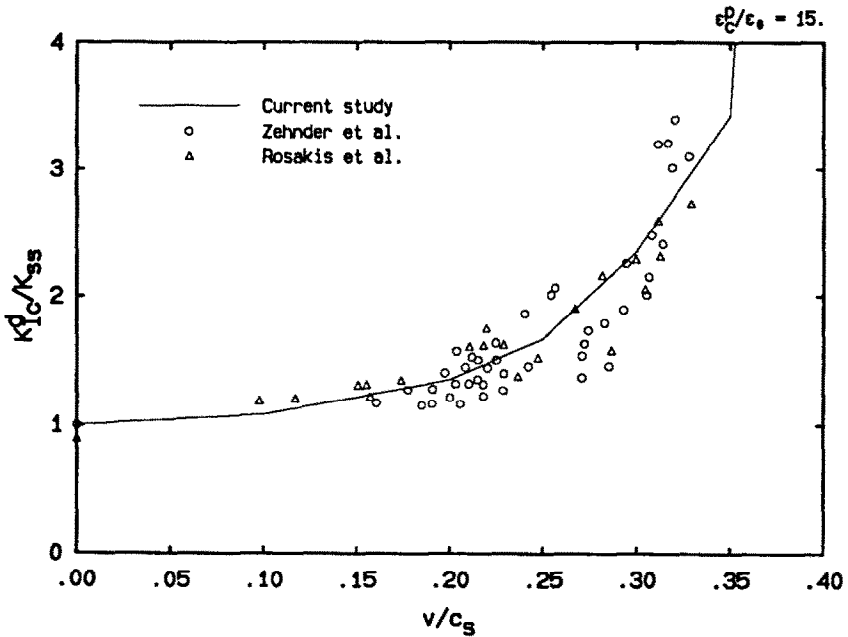


FIG. 20. Comparison of the theoretical  $K_{Ic}^d$  vs  $v$  relation for  $\epsilon_c^p / \epsilon_0 = 15$  with the experimental results by ROSAKIS *et al.* (1984) and by ZEHNDER and ROSAKIS (1990).

experiments conducted on thin 4340 steel specimen of different geometries and under different loading conditions. The 4340 structural steel is however heat treated to yield effective stress-strain relations which can be approximately described as elastic perfectly plastic. The theoretical crack velocity dependence of the dynamic fracture toughness is obtained with the critical effective plastic strain equals to  $15\varepsilon_0$ . It is seen from Fig. 20 that the one-parameter theoretical curve fits the whole experimental data amazingly well. This fact seems strongly to suggest that under small-scale yielding conditions the  $K$ -criterion can still be used to characterize dynamic crack propagation in materials which fracture in a locally ductile manner.

If the above calculation is performed between a quasi-static solution and a stationary solution using the same critical plastic strain value, then the ratio between the fracture toughness for fracture initiation and the toughness for steady-state quasi-static crack growth can be obtained. For example, if we use our quasi-static solution and the solution by NARASIMHAN and ROSAKIS (1988) for the stationary case, the fracture initiation toughness will be approximately 0.62 times the quasi-static steady-state crack growth value  $K_{ss}$ , if  $\varepsilon_0^p/\varepsilon_0$  is taken to be 15.

#### ACKNOWLEDGEMENTS

The authors would like to thank Prof. J. HALL and Dr. S. KRISHNASWAMY for helpful discussions. This study is made possible by an ONR grant through Contract Nos. N00014-85-K-0596 and N00014-90-J-1340. The finite element computation is carried out on the Cray X/MP and SCS-40 computers of the San Diego Supercomputer Center, which was made possible through the Presidential Young Investigator Award (NSF Grant MSM-84-51204) to A.J.R.

#### REFERENCES

- |                                   |       |  |
|-----------------------------------|-------|--|
| ACHENBACH, J. D. and LI, Z. L.    | 1984a | Plastic deformations near a rapidly propagating crack tip. Report NU-SML-TR-No. 84-1, Department of Civil Engineering, Northwestern University, Evanston, IL 60201.    |
| ACHENBACH, J. D. and LI, Z. L.    | 1984b | In <i>Fundamentals of Deformation and Fracture</i> (edited by B. A. BILBY <i>et al.</i> ). Cambridge University Press, Cambridge.                                      |
| ASTM STP 527                      | 1974  | American Society for Testing and Materials.  |
| DEAN, R. H.                       | 1983  | In <i>Elastic-Plastic Fracture: Second Symposium</i> . ASTM STP 803, American Society for Testing and Materials.   |
| DEAN, R. H. and HUTCHINSON, J. W. | 1980  | In <i>Fracture Mechanics: Twelfth Conference</i> . ASTM STP 700, American Society for Testing and Materials.   |
| DENG, X.                          | 1990  | Dynamic crack propagation in elastic-plastic solids. Ph.D. Dissertation, Caltech, Pasadena, CA 91125.  |
| DENG, X. and ROSAKIS, A. J.       | 1990  | Negative plastic flow and its prevention in elasto-plastic finite element computation, to appear in a special issue of <i>Finite Elements in Analysis and Design</i> . |

- DOUGLAS, A. S. 1981 Dynamic fracture toughness of ductile materials in antiplane shear. Ph.D. Dissertation, Brown University, Providence, RI 02912.
- DOUGLAS, A. S., FREUND, L. B. and PARKS, D. M. 1981 In *Advances in Fracture Research* (edited by D. FRANCOIS *et al.*). Pergamon Press, Oxford.
- DUNAYEVSKY, V. and ACHENBACH, J. D. 1982 *Int. J. Solids Struct.* **18**, 1.
- ERDÉLYI, A. 1956 *Asymptotic Expansions*. Dover Publications, New York.
- FREUND, L. B. 1990 *Dynamic Fracture Mechanics*. Cambridge University Press, Cambridge.
- FREUND, L. B. and DOUGLAS, A. S. 1982 *J. Mech. Phys. Solids* **30**, 59.
- GAO, Y. C. 1985 *Int. J. Fracture* **29**, 171.
- GAO, Y. C. 1987 *Int. J. Fracture* **34**, 111.
- GAO, Y. C. and NEMAT-NASSER, S. 1983 *Mech. Mater.* **2**, 47.
- IRWIN, G. R. 1956 In *The Sagamore Research Conference Proceedings*, Vol. 2, p. 289.
- KALTHOFF, J. F. 1983 In *Workshop on Dynamic Fracture* (edited by W. G. KNAUSS *et al.*). Caltech, Pasadena, CA 91125.
- KOBAYASHI, T. and DALLY, J. W. 1977 In *Fast Fracture and Crack Arrest*. ASTM STP 627, American Society for Testing and Materials.
- LAM, P. S. and FREUND, L. B. 1985 *J. Mech. Phys. Solids* **33**, 153.
- LEIGHTON, J. T., CHAMPION, C. R. and FREUND, L. B. 1987 *J. Mech. Phys. Solids* **35**, 541.
- LUO, X., ZHANG, X. and HWANG, K. 1984 In *Proc. ICF Internal Symp. Fracture Mechanics*, pp. 138–145. Science, Beijing, China.
- MCCLINTOCK, F. A. and IRWIN, G. R. 1964 In *Fracture Toughness Testing and Its Applications*, p. 84. ASTM STP 381, American Society for Testing and Materials.
- NARASIMHAN, R. and ROSAKIS, A. J. 1988 *J. Mech. Phys. Solids* **36**, 77.
- NARASIMHAN, R., ROSAKIS, A. J. and HALL, J. F. 1987 *J. Appl. Mech.* **54**, 838.
- PONTE-CASTAÑEDA, P. 1986 *J. Appl. Mech.* **53**, 831.
- RAVI-CHANDAR, K. 1982 An experimental investigation into the mechanics of dynamic fracture. Ph.D. Dissertation, Caltech, Pasadena, CA 91125.
- RAVI-CHANDAR, K. and KNAUSS, W. G. 1987 *J. Appl. Mech.* **54**, 72.
- RICE, J. R. 1967 In *Fatigue Crack Propagation*. ASTM STP 415, American Society for Testing and Materials.
- RICE, J. R. 1968 In *Fracture, An Advanced Treatise*, Vol. II (edited by H. LIEBOWITZ). Academic Press, New York.
- RICE, J. R. 1982 In *Mechanics of Solids* (edited by H. G. HOPKINS *et al.*). Pergamon Press, Oxford.
- RICE, J. R., DRUGAN, W. J. and SHAM, T. L. 1980 In *Fracture Mechanics: Twelfth Conference*. ASTM STP 700, American Society for Testing and Materials.
- RICE, J. R. and SORENSEN, E. P. 1978 *J. Mech. Phys. Solids* **26**, 163.
- RICE, J. R. and TRACEY, D. M. 1973 In *Numerical and Computer Methods in Structural Mechanics* (edited by S. J. FENVES *et al.*). Academic Press, New York.

- ROSAKIS, A. J., DUFFY, J.  
and FREUND, L. B. 1984 *J. Mech. Phys. Solids* **32**, 443.
- SCHREYER, H. L., KULAK, R. F.  
and KRAMER, J. M. 1979 *J. Press. Vess. Technol.* **101**, 226.
- SLEPYAN, L. I. 1976 *Izvestiya Akademii Nauk SSSR, Mekhanika Tver-  
dogo Tela* (English translation) **11**(2), 144.
- SORENSEN, E. P. 1978 *Int. J. Fracture* **14**, 485.
- TRACEY, D. M. 1976 *J. Engng Mater. Technol.* **98**, 146.
- ZEHNDER, A. T. and  
ROSAKIS, A. J. 1990 *Int. J. Fracture* (to appear).